



UNITED STATES
NUCLEAR REGULATORY COMMISSION
WASHINGTON, D.C. 20555-0001

Mr. Kevin Couch
Project Manager
MANDEX, Inc.
12500 Fair Lakes Circle, Suite 300
Fairfax, VA 22033-3804

SUBJECT: ACCOLADE FOR DR. GERRY L. STIREWALT, MANDEX'S TECHNICAL LEAD/SUPERVISOR IN CRADAL, FOR WORK PERFORMED IN SUPPORT OF THE NATIONAL PROGRAM FOR DISPOSAL OF HIGH-LEVEL RADIOACTIVE WASTE IN 1998

Dear Mr. Couch:

This is a letter of commendation, an accolade, for Dr. Gerry L. Stirewalt of MANDEX, Inc., in recognition of the superior technical support that he personally provided to the NRC staff in the course of his duties that demonstrated the highest levels of professionalism.

Dr. Stirewalt was the principal person in CRADAL providing technical support to the Structural Deformation and Seismicity (SDS) team (of which I am co-lead) for its review of the Department of Energy's (DOE's) 3D Geologic Framework Model (GFM3.0) of Yucca Mountain, Nevada, which was due to be completed September 30, 1998. The GFM3.0 code is embedded in the EarthVision software of DGI, Inc., for which Dr. Stirewalt is MANDEX's expert-in-residence. Dr. Stirewalt began his involvement in the GFM3.0 review last spring when he took the lead (working with Jim Thomas of NRC) in helping NRC identify and understand the system requirements of the evolving DOE computer model to recommend the appropriate computer system for operating the rapidly changing EarthVision code. This involved communicating with the key DOE modeler to determine the vagaries of the various choices of hardware, memory specifications, and the like, contacting key DGI personnel, and testing the various existing pieces of equipment and memory supplements. His on-top-of-the-situation technical know-how enabled NRC to procure the right stuff and facilitated Dr. Stirewalt's getting GFM3.0 up-and-running.

The NRC Headquarter's EarthVision system must be compatible with that of its R&D center in San Antonio, the Center for Nuclear Waste Regulatory Analyses (Center). This goal was achieved by Dr. Stirewalt. He used his prior knowledge of the Center staff and computer operations to quickly and smoothly attain Headquarters-Center joint operational compatibility. This achievement, not a small feat by phone, fax, e-mail and post, was done with little direction from the staff. Dr. Stirewalt's actions were self-motivated, persistent, and included all necessary steps to get the job done.

NRC FILE CENTER COP

A subsequent step was to have a face-to-face technological exchange among DOE, Center, and NRC staffs so that the DOE GFM3.0 expert could: (1) instruct the NRC and Center experts on how the model was built; and (2) demonstrate the operation of the code so that NRC and Center could perform various tests and manipulations and eventually evaluate the DOE model. The venue for the two-day exchange was the CRADAL. Dr. Stirewalt made the arrangements for the public meeting in the CRADAL. The exchange, held in May, was a great success, and,

11
NHXT
102

99-149

as a result, Dr. Stirewalt and his counterpart at the Center became experts on DOE's model and its underpinnings. This was a prerequisite for the ultimate task of evaluating the model by the end of September, an extraordinary effort that I will briefly describe in a following paragraph.

Dr. Stirewalt is a superb communicator. He is well-organized to the extent of following-up by e-mail, or by hand-delivered notes, on the progress of activities that involve the CRADAL in which he and I have been involved. However, the GFM3.0 task required official communication with a potential NRC applicant, an NRC contractor, and NRC staff on a public matter of potential significance to licensing. Accordingly, he invariably notified me of his intentions to communicate with DOE and Center staff, as needed, and in his communications was always clear and sensitive so as not to give the impression that he was speaking on behalf of NRC staff. Also, he frequently sent status reports of pending actions with effective reminders of what is needed for resolution. He upheld the highest standards of openness, politeness, and efficiency. Working with Dr. Stirewalt continues to be a pleasure, in part, because he is always ready to act, always on top of the situation, and keeps me informed - he's effective.

Dr. Stirewalt's geological expertise was invaluable in suggesting explanations of apparent discrepancies between NRC and DOE model results. Also, he took several initiatives in conducting tests on DOE's model. For example, he conducted a test of the model that required detailed knowledge of EarthVision's structure-building procedure. His conclusions, combined with that from the Center, led to a recommendation to NRC management that it adopt GFM3.0 and adapt it for its own use. This recommendation was accepted. The hard parts of the job were completed without fanfare, without getting me involved unduly in day-to-day problems and decisions that arose in doing this pioneering work for NRC.

Dr. Stirewalt was able to put his skills to work for NRC to accomplish extraordinary feats when NRC management indicated that it wanted the results of the GFM3.0 review seamlessly incorporated into the SDS Issue Resolution Status Report. That meant scrapping the informal final report of the review (previously for internal NRC use only) and re-drafting the text and figures in a totally different format for distribution to DOE and the public (see enclosure). Only Dr. Stirewalt's willingness, efforts, and skills ensured that the request would be met on time. He was key to the successful production of the report because he was responsible for: (1) compiling and editing the first draft of the two-part report; and (2) production of the illustrations of the 3D models generated at the Center and CRADAL. In accelerating the production of the GFM3.0 review to meet the new format, Dr. Stirewalt worked tirelessly on the graphics and text changes (working closely with a production secretary) to overcome myriad obstacles, such as: (1) conforming Center and NRC text styles; (2) scale changes; and (3) multiple multi-colored prints from the CRADAL.

Dr. Stirewalt's unique combination of expertise in geology and experience in 3D computer modeling, plus his willingness to work as long and as hard as it takes, without complaint, to complete an important task, enabled NRC to exceed its planned goal. It is my considered opinion that without Dr. Stirewalt's skills, efforts, and dedication - his professionalism - the bases for decision and feedback to DOE would not have been as complete and of such high quality as the results shown in the enclosure. His immense contributions to the success of the GFM3.0 review enhanced MANDEX's reputation.

He is to be commended highly for his superior technical support and creative writing and the manner in which he performed them.

Sincerely yours,



Philip S. Justus
Senior Geologist and SDS Co-lead
Division of Waste Management
Engineering and Geosciences Branch

cc: Michael Bell, NRC
James Thomas, NRC
William Reamer, NRC
King Stablein, NRC
David Brooks, NRC
Isaac Kirk, Jr., NRC

Enclosure: Review of U.S. Department of Energy's Geologic Framework Model, Version 3.0 (GFM3.0):" Appendix F, in Issue Resolution Status Report - Key Technical Issue: Structural Deformation and Seismicity, Rev. 1, U.S. Nuclear Regulatory Commission, September 1998 {G. Stirewalt's co-authorship appears in the 'Acknowledgments' section}

He is to be commended highly for his superior technical support and creative writing and the manner in which he performed them.

Sincerely yours,

Original Signed By

Philip S. Justus
 Senior Geologist and SDS Co-lead
 Division of Waste Management
 Engineering and Geosciences Branch

cc: Michael Bell, NRC
 James Thomas, NRC
 William Reamer, NRC
 King Stablein, NRC
 David Brooks, NRC
 Isaac Kirk, Jr., NRC

Enclosure: Review of U.S. Department of Energy's Geologic Framework Model, Version 3.0 (GFM3.0): Appendix F, in Issue Resolution Status Report - Key Technical Issue: Structural Deformation and Seismicity, Rev. 1, U.S. Nuclear Regulatory Commission, September 1998 {G. Stirewalt's co-authorship appears in the 'Acknowledgments' section}

DISTRIBUTION: File Center

DOCUMENT NAME:

OFC	ENGB	ENGB	ENGB					
NAME	PSJustus:cc	DJBrooks	CWReamer					
DATE	12/01/98	12/01/98	12/01/98					

OFFICIAL RECORD COPY

APPENDIX F

REVIEW OF U.S. DEPARTMENT OF ENERGY'S GEOLOGIC FRAMEWORK MODEL, VERSION 3.0 (GMF3.0)

[Constructed using EarthVision software, Version 4.0, by R. Clayton, M&O, Las Vegas, Nevada]

The need to review GFM3.0, and a summary of events that led to the review, can be found in a letter from M. Bell to S. Brocoum dated September 30, 1998, subject: "Review of U.S. DOE's GFM3.0 - A Step in the Review of DOE's ISM." The staff had committed to review DOE's ISM2.0 by the end of FY98, at DOE's request. DOE notified the staff, early in its review, that ISM3.0 was under development and would be issued at the end of the first quarter of FY99. The staff were also informed that ISM3.0 was to be based on GFM3.0 which was to be issued in the second quarter of FY98. Therefore, NRC refocused its 3D model review resources from ISM2.0, and targeted GFM3.0 to be reviewed as a necessary first step toward the goal of a review of ISM3.0. This appendix provides a discussion and results of the GFM3.0 review.

OBJECTIVES OF THIS REVIEW

- (1) To test and evaluate GFM3.0 for DOE's purposes of representing site stratigraphy and faults as a framework for its Integrated Site Model, Version 3.0;
- (2) To evaluate GFM3.0 as a necessary step toward the evaluation of adequacy of DOE's ISM3.0; and
- (3) To consider replacing NRC's EarthVision geologic site model with an adapted version of GFM3.0 as NRC's 3D-model of the site, for independent NRC analyses.

STRUCTURE OF THE REVIEW AND CREDITS

The review, tests, and evaluations of GFM3.0 were conducted cooperatively by staff from the Center for Nuclear Waste Regulatory Analyses (CNWRA), located in San Antonio, Texas, and from MANDEX, Inc., located at NRC Headquarters, under the direction of NRC staff. The review was organized as follows:

- (1) Introduction and Summary of CNWRA and MANDEX Results
- (2) Part I - Analysis of Stratigraphic Horizons in GFM3.0
 - (i) Tests and Evaluation of Stratigraphy and Topography
- (3) Part II - Analysis of Faults in GFM3.0
 - (i) Tests and Evaluation of Faults and Fault Blocks
 - (ii) Evaluation of Selected Geologic Cross Sections

SUMMARY OF QUESTIONS USED TO FOCUS THE ANALYSIS OF GFM3.0

The questions are enumerated here to introduce the scope of the analyses in Parts I and II:

- Are the data used for defining subsurface horizons (Pt.I, question (Q) 1) and faults at the surface and in the subsurface (Pt.II, Q 1) in GFM3.0 deemed appropriate and sufficient for these purposes?
- Do the model horizon surfaces (Pt.I, Q 2) and fault traces and fault surfaces (Pt.II, Q 2) as modeled in GFM3.0 fit the input data?
- Were all essential data for constructing GFM3.0 provided in the data files that accompanied the model (Pts. I and II, Q 3)?
- Are alternative interpretations of data warranted (Pts. I and II, Q 4)?
- Is it possible to incorporate reasonable alternative interpretations of subsurface fault geometry into GFM3.0, specifically the interpretation that certain faults are non-planar and merge with or terminate against major structures at depths of less than -8000 feet above the base of GFM3.0 (Pt.II, Q 5)?
- What observations were made relative to representation of horizons (not a separate question in Part I) and faults (Pt.II, Q 6) in GFM3.0 that may require further explanation or clarification?

SUMMARY OF OBSERVATIONS OF GFM3.0

Parts I and II describe both the merits and observations of GFM3.0. Some observations that may require explanation or clarification prior to completion of the staff review of ISM3.0 in FY99 are as follows:

- (1) Stratigraphy and the Paleozoic surface are not well constrained at depth or at the edges of the model;
- (2) Topographic elevations over about 85% of the model area have elevation differences of less than 5 meters (comparing two sources of elevation data). Such differences are not detrimental because topography was not used to control subsurface stratigraphy;
- (3) All stratigraphic borehole controls assume no deviation of boreholes from the vertical;
- (4) Mismatches between true and modeled elevations of subsurface horizons typically are less than 25 feet, although a few are greater than 50 feet. Possible explanations for these mismatches include new realizations of fault dips at depth, presence of unmapped faults, or results of sparse data;
- (5) A structure in Antler Wash shown on the USGS central block geologic map may need to be added to the model to help explain the hydrogeologic tracer data from C-wells;
- (6) The imbricate fault zone is presently modeled as a single fault. This representation may need to be changed if it is necessary to understand or explain phenomena in that zone;
- (7) Warping or folding of horizons in the hangingwall of faults is unexplained by the presence of planar faults;
- (8) Boomerang Point fault shows an apparent reversal of slip sense which may need to be explained;

- (9) Dune Wash fault is shown truncated against the Ghost Dance fault in one cross section, but not in sections to the north or south, and the surface traces of the two faults do not appear to intersect. This observation may need to be explained;
- (10) Many faults are shown with increasing displacements with depth, suggesting that they are growth faults. This may need to be explained and compared with other DOE models of fault development. However, poorly constrained stratigraphic horizon data in the northern and southern edges of the model may be an important factor;
- (11) Complex fault interactions have been modeled at depth in some zones - a positive feature of the model. Some of the structural relationships shown, such as one fault 'beheading' another, has implications for understanding past, and perhaps future, faulting and may need to be explained in more detail.

SUMMARY OF RESULTS

The objectives of this review of GFM3.0, stated above, were met as follows, respectively:

- (1) The staff considers GFM3.0 to be adequate for representing the stratigraphy, faults, fault blocks, geologic cross sections, and topography of Yucca Mountain at the site scale;
- (2) The staff considers GFM3.0 to be an adequate stratigraphic, fault and fault block framework for DOE's ISM3.0, to the extent of the staff's understanding of the scope of ISM3.0 (e.g., D. Bryan, Translation and Use of GFM3.0, Handout at DOE/NRC Quarterly Technical Meeting, June 18, 1998).
- (3) The staff considers an adapted version of GFM3.0 adequate for NRC's needs in conducting 3-D analyses of the Yucca Mountain site, including reviews of subsequent ISMs.

The staff have made certain observations of the model that may require explanation or clarification, particularly to enable the staff to fully evaluate ISM3.0. The illustrated evaluations of stratigraphy (50 surfaces, including alluvium), faults (42 surfaces), fault blocks (43 included), topography and geologic cross sections detailed in Parts I and II of this appendix, in the following two parts, are the source for observations made during this review. The observations notwithstanding, GFM3.0 was considered adequate for its intended uses. Note that the following analyses were not performed for this review: (1) a critique of the quality assurance or quality control of data; and (2) a critique of the planar fault model used by DOE.

PART I - ANALYSIS OF STRATIGRAPHIC HORIZONS IN GFM3.0

1. Are the raw data appropriate and sufficient for defining subsurface horizons?

Horizons in GFM3.0 were derived from several data sources, including the EG&G digital topographic model (personal communication with R. Clayton, July 1998), the geologic map of Day and others (1997), well log horizon picks, and geophysical gravity data. These data were combined in an EarthVision geologic model that presents an interpretation of the stratigraphic units in the vicinity of the proposed repository. The relatively small number of wells and limited geophysical data sets available to the modelers necessitates an increased level of reliance on the surface geologic map to establish shallow horizon relationships that are then confirmed at depth by geophysical well logs. The deeper model horizons, i.e., Tund and Paleozoic, are not well-sampled with boreholes and were, in part, interpreted from gravity measurements. Thus, any utilization of GFM3.0 horizon data in other modeling and/or design work should be undertaken with an understanding of the accuracy of the input data and the extent to which GFM3.0 honors these data.

This analysis of GFM3.0 assumes the well log horizon picks used in building the model have been qualified by an appropriate quality process. Thus, the question addressed in this analysis is whether there are sufficient data on which to build the subsurface horizons, and whether they have been honored. Figure 1 contains an image taken from GFM3.0 showing the location of the boreholes incorporated in the model. There is a higher density of wells in the center of the model than at the model edges. Thus, the stratigraphic units at the model boundaries are the result of data extrapolation calculations by the EarthVision software application used to create GFM3.0.

2. Do model horizon surfaces fit the data?

Prior to validating the horizon ties with the borehole picks, CNWRA performed a brief comparison of the DOE and CNWRA topography models. DOE has utilized a topography model produced by EG&G with a 100-foot grid node spacing. The CNWRA uses USGS 7.5 minute digital elevation models with a 30-meter grid node spacing. After making the appropriate coordinate system conversions, the CNWRA topography model was subtracted from the DOE model, yielding a difference plot shown in Figure 2. Approximately 85 percent of the elevation differences are less than 5 meters. These differences are not considered to be significant to GFM3.0 because the topography model is used to truncate stratigraphic units at the model surface. The topography was not used to control or influence the subsurface stratigraphy.

A subsurface horizon tie analysis was performed by CNWRA to measure the agreement between borehole horizon picks and modeled horizon depths. The tie analysis compares the depth at which the borehole actually intersected a horizon and the modeled depth for that same coordinate. Borehole deviation logs were not available to CNWRA at the time this analysis was performed. All comparisons assume undeviated wells. The data processing sequence used to generate the tie analysis was:

- A. Extract individual horizon surfaces using the EarthVision, Geologic Structure Builder, Horizon Export utility.
- B. Compute the borehole-horizon intersection coordinate for each well penetrating the horizon. Repeat this process for several horizons in the stratigraphic column.

GFM with Well Locations

Zone Color Key
 Display: gfm3b_ft_sliced_faces

59	alluvium
58	Root/Infiltration
48	Thin_Rainier
47	Top2
46	Top1D
45	Top2
44	Top2
43	Top1
42	Top1
41	Top1
40	Top1 & 2
39	Top1
38	Top2
37	Top2
36	Top2
35	Top1
34	Top1
33	Top1
32	Top1
31	Top1
30	Top1
29	Top1
28	Top1
27	Top1
26	Top1
25	Top1
24	Top1
23	Top1
22	Top1
21	Caliche
20	Caliche
19	Proven
18	Proven
17	Proven
16	Proven
15	Proven
14	Ballstrop
13	Ballstrop
12	Ballstrop
11	Ballstrop
10	Ballstrop
9	Tramuc
8	Tramuc
7	Tramuc
6	Tramuc
5	Tramuc
4	Tramuc
3	Tramuc
2	Tramuc
1	Palaeozoic

Z exaggeration: 1.0
 Azimuth: 328.1
 Inclination: 33.7
 X Front Cut: 547000.0
 Y Front Cut: 739000.0
 Z Front Cut: 6000.0

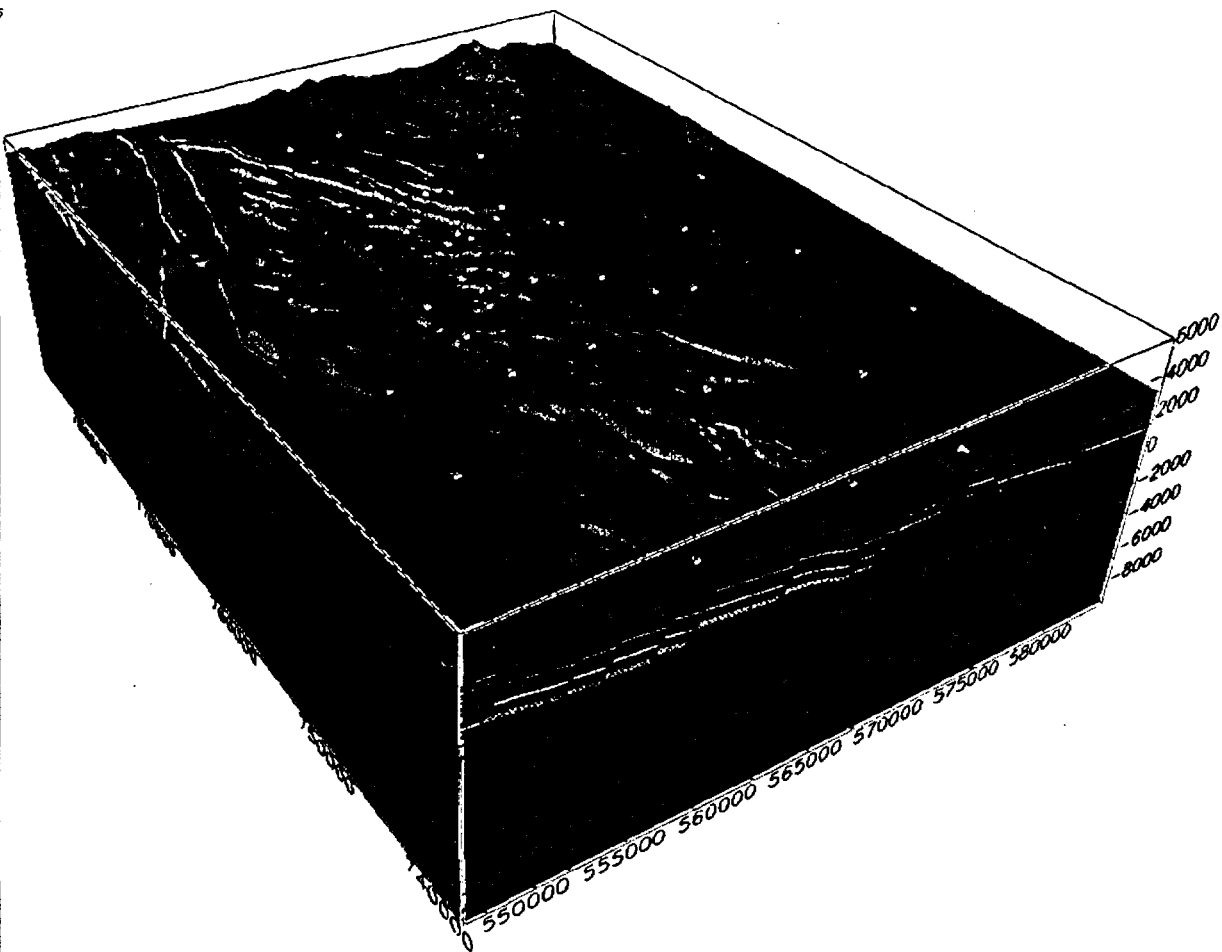


Figure 1 - Example view of GFM 3.0 with input borehole locations shown as gray cubes

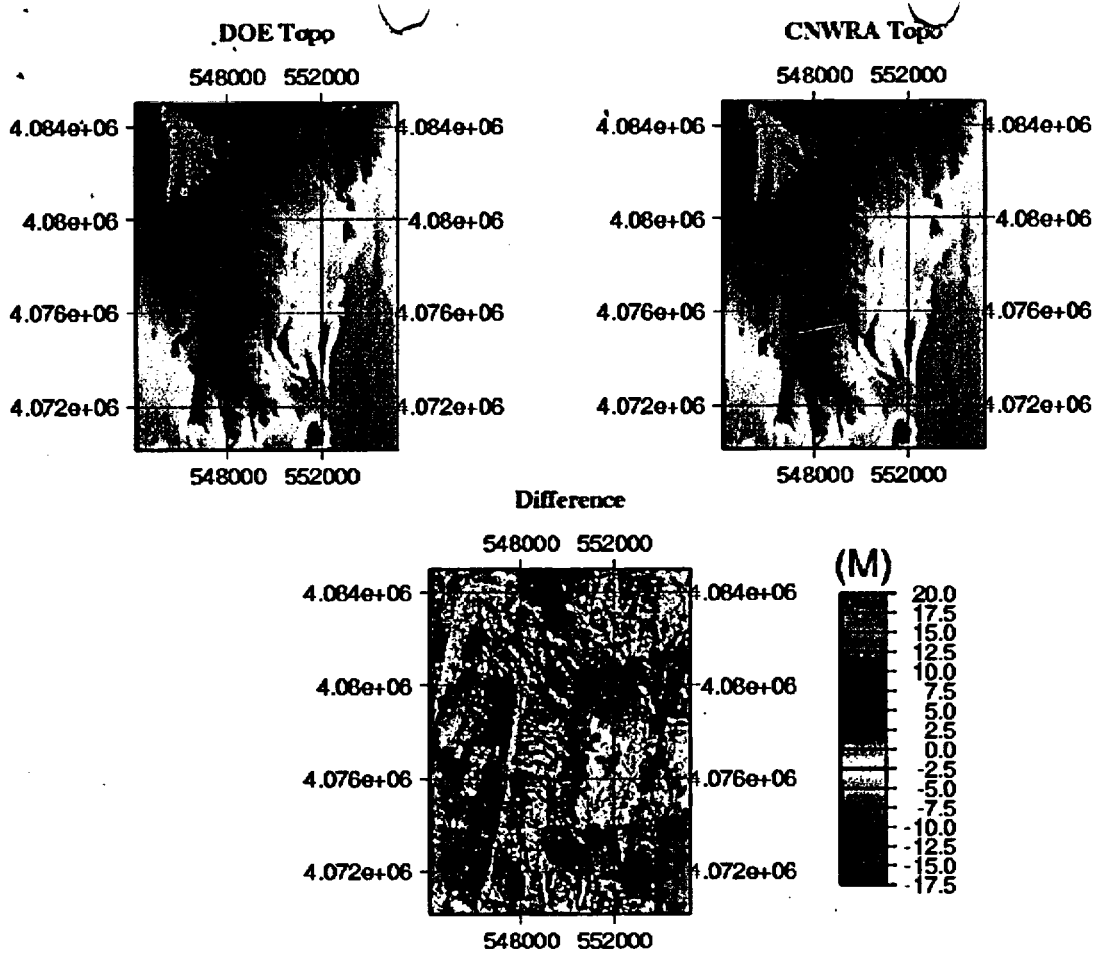


Figure 2 - Comparison of the DOE and CNWRA digital elevation models

C. Compare the extracted horizon elevations with the elevations picked from the well logs.

Table 1 contains the original well picks provided by DOE for the ten horizons used in this analysis. Table 2 contains the modeled horizon elevations, and Table 3 contains the difference between the well log picks and modeled elevations.

The results in Table 3 show discrepancies between the true and modeled elevations that are typically less than 25 feet. A few discrepancies greater than 50 feet warranted further investigation to determine if the discrepancies are the result of insufficient data control, inaccurate input data, or side effects from non-vertical faulting.

In computing the subsurface horizon models, EarthVision employs numerical algorithms that attempt to fit a surface to the control points established by the well log horizon picks and fault structures. The quality, number, and spatial distribution of data points all effect the accuracy with which the model surface fits the input data. In areas of poor data control, the software algorithms tend to produce smooth surfaces that follow general trends established by the sparse control points. Likewise, the software attempts to honor the majority of densely spaced data points, but outliers may have been disregarded by EarthVision if they fell outside the software parameter ranges specified by the DOE modelers. One approach to analyzing these discrepancies is to plot the model-well discrepancies on a three-dimensional representation of the horizon surface (Figure 3). This type of plot allows the viewer to examine the relationships between model-well miss-ties, well density and spatial distribution, and faulting.

Figure 3 contains a 3-D view of the upper vitrified Tram unit with the model-well discrepancies plotted as color-filled contours. The legend on the left side of the plot defines the miss-tie range as plus/minus 100 feet. The gray boxes above the model surface represent the locations of the well log data that were used as control points for computing the horizon elevations. The red circular region in the vicinity of the C#2 well represents a model-well mismatch of -53 feet. This means the EarthVision software computed the elevation of the horizon to be 53 feet higher than the geologist picked the horizon location on the C#2 well logs. Only 14 well control points were available for the computation of this Tram unit, and Figure 3 illustrates that the C#2 well is not surrounded by wells having smaller model-well miss-ties. Thus, one cannot confidently say that the C#2 well log pick is bad and has been disregarded by the EarthVision software as an outlier. A case could be made that: (1) the -53 foot C#2 discrepancy is the result of insufficient data to constrain the EarthVision software; or (2) that the fault structure in the GFM3.0 model has resulted in the C#2 well being located on the wrong side of a fault. Figure 3 shows the C#2 well in very close proximity to the Midway fault, which may possibly be explained by an incorrect assumption that: (1) the C#2 well is not deviated; or (2) that the subsurface control on the Midway fault is incorrect.

Figure 4 shows discrepancies of +117 and -56 feet where the WT-7 and WT#14 wells intersect the Calico horizon near the SolWest and Paintbrush faults, respectively. Figure 5 also shows +59 and -88 foot discrepancies for the WT-7 and WT#14 wells intersecting the Tptpl unit. Again, it may be possible to ascribe the discrepancies to incorrect borehole placement or inaccurate subsurface fault control. However, the -117 foot discrepancy for the WT#6 well in Figure 5 is not as easily explained because a fault surface is not present in the vicinity of the borehole. This disagreement may possibly be explained as a data outlier, poorly constrained software calculations, or the presence of an unmapped fault.

Table 1 - DOE Well Log Horizon Picks (ft)

#wellid	Tpcpv3	Tpbt4	Tpp	Tptpul	Tptpl	Tptpv3	Tac	Tcpm	Tctuv	Tund
a#4	119	151	197							
a#5	128	149	180	475						
a#6	125	144	186	422						
b#1				440	765	1283	1385	1992	2883	3960
c#2				457	725	1205	1335	1773	2725	
G-1			135	457	815	1287	1426	1920	2639	3558
G-2	225	235	494	977	1280	1634	1757	2705	3574	3982
G-3	348	373	392	548	830	1187	1413	1663	2637	3876
G-4	118	141	168	420	774	1317	1409	1880	2756	
H-1				538	897	1410	1505	1969	2730	3661
H-3	370	400	417	540	848	1194	1400	1640	2477	3637
H-4	174	193	216	376	703	1185	1317	1746	2664	3819
H-5	404	438	471	741	1088	1582	1705	2085	2742	3422
H-6				435	795	1213	1356	1602	2258	2878
J#13	587	629	650	801	1003	1300	1482	1848	2358	3220
NRG#1										
NRG#2	276									
NRG#4	318	338	375	700						
NRG#5	140	163	215	565	902					
NRG-6	135	159	175	466	810					
NRG-7A	70	102	172	518	878	1415	1498			
ONC#1	578	597	621	810			1274			
p#1				248	640	1090	1270	1535	2262	2863
SD-7	305	326	343	490	803	1182	1406	1765	2598	
SD-9	57	92	156	473	846	1358	1480	1939		
SD-12	240	264	278	470	787	1278	1412	1787		
UZ-1			105	470	830					
UZ#4	71	99	174							
UZ#5	89	118	186							
UZ-6	383	433	450	610	917	1333	1460	1750		
UZ-7A	164	198	215		607					
UZ-14							1420	1850		
UZ#16	141	161	189	371	669	1108	1197	1571		
WT-1	395	431	446	593	888	1299	1384			
WT-2	193	227	247	421	727	1179	1319	1706		
WT#3					11	189	358	660		
WT#4	261	281	324	660	785	1091	1156			
WT#6					250	303	383			
WT-7	344	370	391	546	959	1287	1438			
WT-10	863	887	924	1049						
WT#11	239	271	287	430	782	1058	1208			
WT#12	297	319	339	478	760	1151	1276			
WT#13	416	440	460	630	868					
WT#14				275	534	1024	1210			
WT#15	332	349	372	641	919					
WT#16	368	386	462	830	830	1013	1068			
WT#17	188	197	217	336	535	874	998	1318		
WT#18	314	340	497	900	1170	1501	1620			

Table 2 - GFM3.0 Horizon Picks Computed With EarthVision (ft)

#wellid	Tpcpv3	Tpbt4	Tpp	Tptpul	Tptpll	Tptpv3	Tac	Tcpm	Tctuv	Tund
a#4	125.7	153.2	199.7	548.2	889	1326	1399.2	1954	2879.3	3889.8
a#5	121.1	143	173.7	466.2	804.4	1297.4	1375.1	1943.3	2869.7	3906.4
a#6	124.4	144	184.1	421.6	765.8	1301.2	1393.7	1929.2	2845.1	3905.4
b#1	227.2	212.7	248.8	491.6	816.4	1332.7	1435.1	2042.4	2903.2	3980.9
c#2	280.1	299.7	322.2	492.8	762.1	1193.9	1324.1	1760.5	2778.3	3410.9
G-1	36.8	38.7	120.1	473.1	832.4	1309.9	1446.9	1940.8	2671	3593.9
G-2	213.3	223	482.6	963	1263.6	1621	1743.1	2690.1	3552.1	3957.4
G-3	350.7	375.1	394.2	550.3	832.9	1187.3	1412.7	1663	2636	3874.9
G-4	106.9	130.3	157.5	412.5	766.3	1310.6	1403.8	1872.8	2748.4	3755.6
H-1	39.1	71.9	169.7	520.9	879	1381	1486.7	1954.8	2716.3	3646.7
H-3	371.3	400.5	417.4	540.7	847.6	1200.1	1408.4	1649.2	2486.5	3649.6
H-4	171.2	190.2	213	373.3	700.6	1178.7	1309.8	1738.2	2650.3	3804.5
H-5	434.7	468.3	502.6	772.6	1120.7	1574.6	1697.4	2075.3	2753.7	3447.9
H-6	241.7	263.5	320.9	486.1	846	1219.8	1362.3	1608.4	2264.4	2886.5
J#13	633.6	675.5	696.4	846.7	1049.3	1296.5	1478.8	1844.4	2352.3	3213.2
NRG#1	264	280.4	310.4	573.6	796.3	1170.6	1286.3	1975.8	2833.6	3757
NRG#2	238.7	252.3	277.8	547.5	764.4	1126.6	1228.1	1927.9	2830.9	3796.9
NRG#4	329.8	349.4	386	708.2	952.3	1341.7	1419.6	2083.1	3082.7	4108.6
NRG#5	135.2	161.8	213.1	566.5	903.6	1329	1401.7	1963	2891.7	3900.7
NRG-6	127.6	151.2	167.4	460.8	805.1	1323.6	1403.9	1931.1	2848.6	3877.3
NRG-7A	60.5	92.9	165.9	510.7	871.3	1411.1	1497.5	1980.3	2804.4	3766
ONC#1	568.2	587.4	610.9	769.9	970.8	1111.7	1246.8	1722.7	2769.9	3620.3
p#1	111.1	127.6	146.9	271.9	667.1	1112.6	1293.4	1554.4	2272.3	2870.9
SD-7	324.7	345.4	362.4	508.3	820.9	1195	1414	1774.5	2595.3	3582.1
SD-9	76.7	110.1	169.3	485.6	854.7	1366.1	1482.8	1943.6	2764.6	3701.3
SD-12	265.1	289.9	304.8	493.4	808.6	1290.3	1423.2	1801.4	2535	3523
UZ-1	24.7	32.9	103.8	465.9	825.9	1298	1420.5	1858.3	2520.6	3382.6
UZ#4	57.7	85.6	160.7	552.9	794.4	1118.3	1189.4	1834.9	2795.4	3776.7
UZ#5	93.4	121.8	188.2	576	816.8	1131.2	1201.9	1849.1	2821.3	3809
UZ-6	386.1	435.3	452.8	612.7	919.9	1346.5	1474.3	1764	2482	3472.7
UZ-7A	107.1	139.9	157.9	331.1	623	1073.4	1212.4	1603.8	2374.7	3479.3
UZ-14	7.2	16.2	85.8	450.5	810.4	1288.6	1407.6	1837.9	2492	3341.5
UZ#16	151.1	170.9	198.9	381.7	678.6	1072.1	1204	1584.9	2558.6	3647.7
WT-1	395.8	431.7	446.7	592.7	887.5	1296.9	1382.4	1720.3	2658.7	3541.4
WT-2	210.4	243.1	262.2	441.8	747.4	1187.9	1318.2	1676.6	2408.6	3420.1
WT#3	13.7	13.7	13.7	13.7	13.7	142.8	311.7	613.6	1244	2035.2
WT#4	285.5	296.3	324.3	628.3	692.6	1040.6	1106.1	1850.4	2856.3	3806
WT#6	250.5	250.5	250.5	338.8	367.2	316.4	397	1462.4	2238.1	2627.2
WT-7	359.1	384.7	406.3	562.2	900.4	1216.1	1320.6	1540.4	2362.7	3425.3
WT-10	884.9	908.9	945.7	1070.7	1469.4	1760	1900.6	2137.8	2985.1	4132.3
WT#11	211.4	243.1	259.3	401.6	753.2	1024.9	1155.8	1361.9	1526.6	2596.6
WT#12	331.7	353.8	373.7	513.1	794.3	1181.3	1305.6	1521.7	2256.6	3123.2
WT#13	413.3	437.1	457	627	866	1234.6	1432.1	1828.8	2369.1	2949.1
WT#14	110.9	128.1	151.8	362.3	621.9	1079.7	1266.2	1769.8	2471.6	3054.1
WT#15	348.8	365.8	388.4	656.5	937.6	1312.9	1437	2262.5	2612.8	3079.2
WT#16	341.5	359.6	438	821.3	821.1	1001.1	1056.8	1890.9	2543.1	3178.5
WT#17	189.3	198.2	218.1	336.8	535.8	875.1	999	1318.8	2227.6	3138.4
WT#18	326.7	352.7	506.5	899.8	1166.8	1503	1617.9	2245	3080	3976

Table 3 - Model-Well Miss-Ties Computed By Subtracting The Model Horizon Elevations In Table 2 From Well Log Horizon Picks In Table 1 (ft)

#wellid	Tpcpv3	Tpbt4	Tpp	Tptpul	Tptpll	Tptpv3	Tac	Tcpm	Tctuv	Tund
a#4	-7	-3	-3							
a#5	7	6	6	9						
a#6	0	0	2	0						
b#1				-52	-51	-50	-50	-50	-21	-21
c#2				-36	-37	11	11	13	-53	
G-1			15	-17	-18	-23	-21	-21	-32	-36
G-2	12	12	12	14	16	13	14	15	22	25
G-3	-3	-3	-3	-2	-3	-1	0	0	1	1
G-4	11	11	11	8	8	6	6	7	7	
H-1				17	18	29	18	14	13	15
H-3	-2	-1	0	-1	1	-6	-8	-9	-10	-13
H-4	3	3	3	3	2	6	7	8	14	14
H-5	-31	-31	-32	-32	-33	7	8	10	-12	-26
H-6				-51	-51	-7	-6	-6	-6	-9
J#13	-47	-47	-46	-46	-46	4	3	4	6	7
NRG#1										
NRG#2	38									
NRG#4	-12	-11	-11	-8						
NRG#5	5	1	2	-2	-2					
NRG-6	8	7	8	5	5					
NRG-7A	9	9	6	8	6	4	1			
ONC#1	10	10	10	40		27				
p#1				-24	-27	-23	-23	-19	-10	-8
SD-7	-20	-20	-19	-18	-18	-13	-8	-10	3	
SD-9	-20	-19	-14	-13	-9	-8	-3	-5		
SD-12	-26	-26	-27	-23	-22	-12	-12	-14		
UZ-1		1		4	4					
UZ#4	14	13	13							
UZ#5	-4	-4	-2							
UZ-6	-3	-3	-3	-3	-3	-14	-14	-14		
UZ-7A	57	58	57	-16						
UZ-14						13		12		
UZ#16	-10	-10	-10	-11	-10	35	-7	-14		
WT-1	-1	-1	-1	0	1	2	2			
WT-2	-17	-16	-15	-21	-20	-9	1	29		
WT#3				-3		46	46	46		
WT#4	-25	-15	0	32	92	50	50			
WT#6				-117		-13	-14			
WT-7	-15	-15	-15	-16	59	71	117			
WT-10	-22	-22	-22	-22						
WT#11	28	28	28	28	29	33	52			
WT#12	-35	-35	-35	-35	-34	-30	-30			
WT#13	3	3	3	3	2					
WT#14				-87	-88	-56	-56			
WT#15	-17	-17	-16	-16	-19					
WT#16	27	26	24	9	9	12	11			
WT#17	-1	-1	-1	-1	-1	-1	-1	-1		
WT#18	-13	-13	-10	0	3	-2	2			

Tramuv 2-D Grid

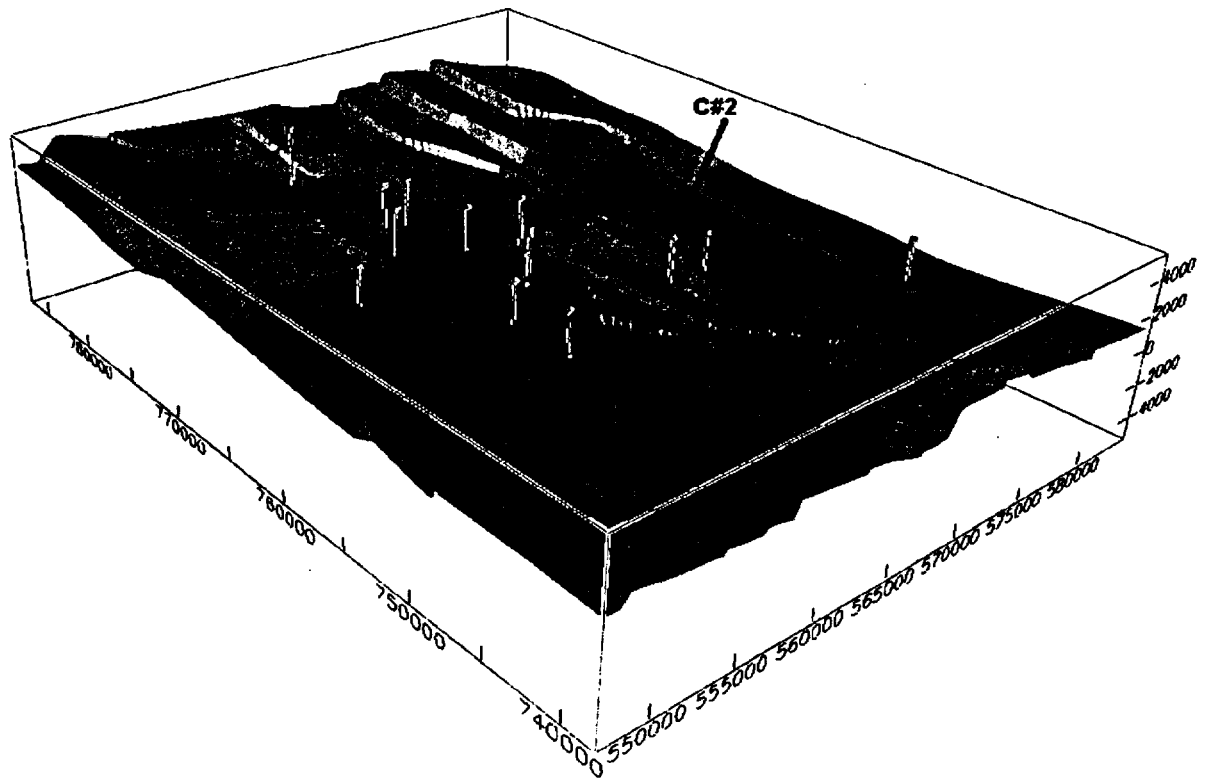
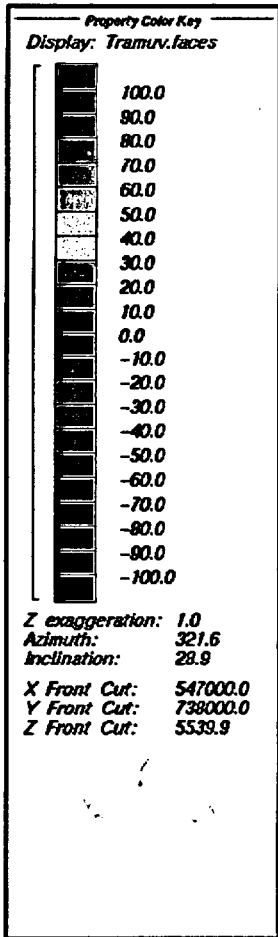


Figure 3 - Tramuv model-well miss-tie analysis plot illustrating the difference between the computed horizon and the picked well-log elevations using color coded contours

Calico 2-D Grid

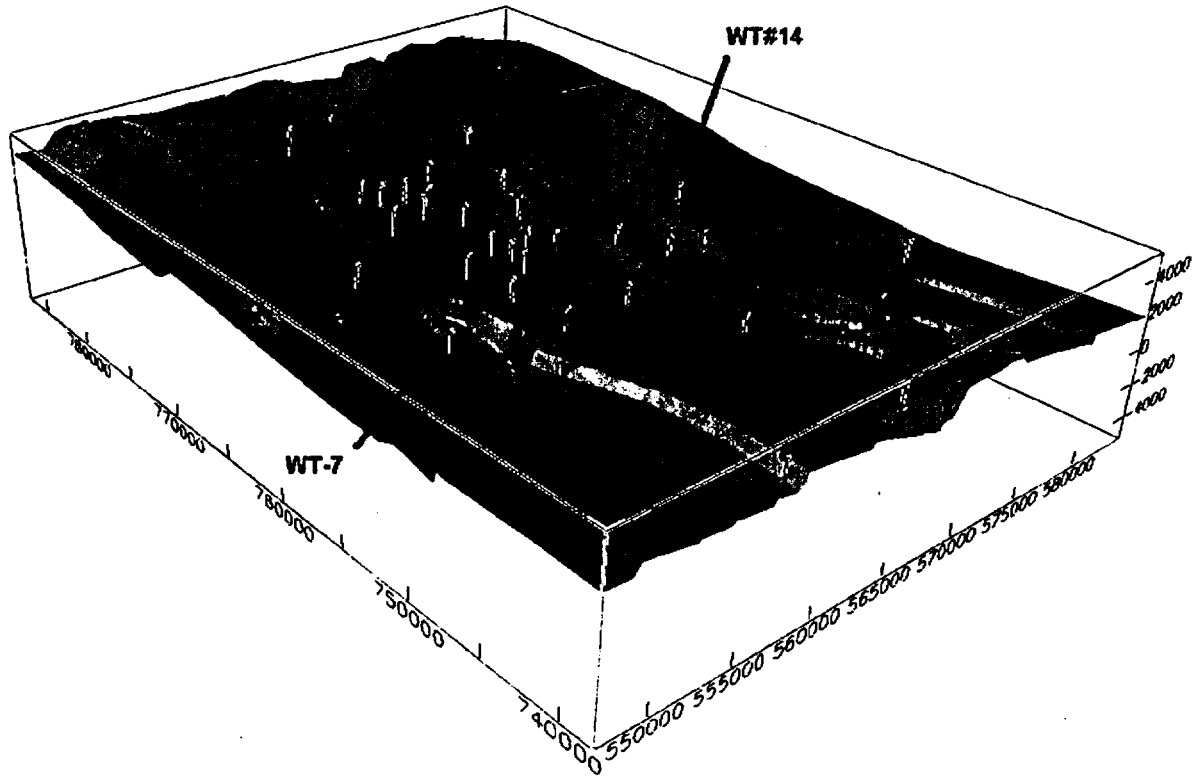
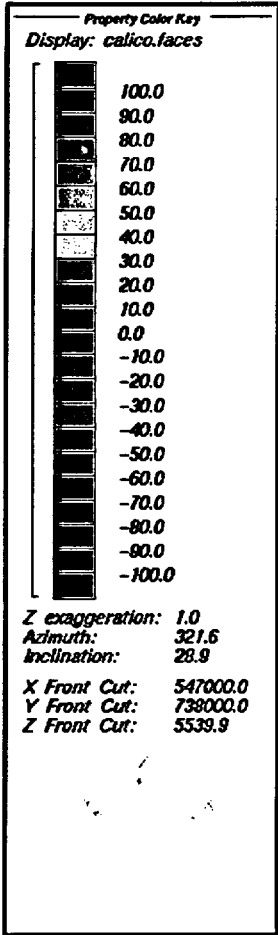


Figure 4 - Calico model-well miss-tie analysis plot illustrating the difference between the computed horizon and the picked well-log elevations using color coded contours

Tptpll 2-D Grid

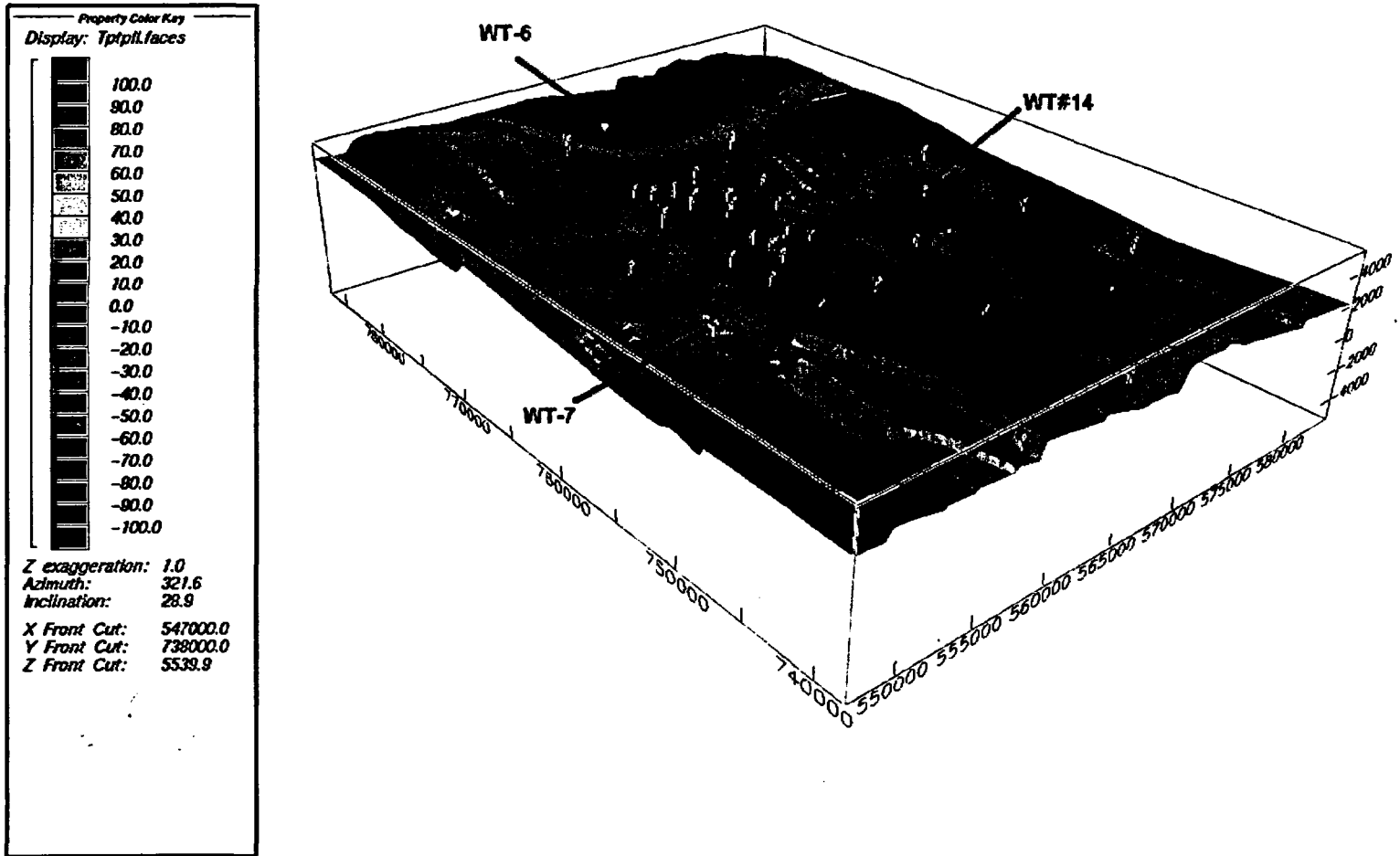


Figure 5 - Tptpll model-well miss-tie analysis plot illustrating the difference between the computed horizon and the picked well-log elevations using color coded contours

3. Were all essential data provided in the data files?

The original release of GFM3.0 omitted a small number of files used by the EarthVision Geologic Structure Builder to create 3-D model files and export individual 2-D horizons. Subsequently, DOE provided these files, as well as the DOE topography model and well log horizon picks. All essential data required to manipulate and analyze GFM3.0 are available.

4. Are alternative interpretations of data warranted?

Construction of GFM3.0 was undertaken using a reference horizon-isochore approach to modeling the subsurface horizon relationships. Alternative approaches to developing GFM3.0, through the use of balanced cross-sections, are possible, but not warranted due to the relatively consistent and small discrepancies between the modeled horizons and the well log horizon picks.

In summary, as new data from wells and the ESF become available, GFM3.0 may be updated as required by the additional data. The integration of deviation data is recommended if the deviation logs identify lateral deviations of more than 10 feet. Some refinement of the fault surfaces may be warranted if model-well discrepancies persist once the deviation data has been analyzed and/or incorporated in GFM3.0.

At this time, there are no major stratigraphic discrepancies that would preclude NRC or DOE from using GFM3.0.

PART II - ANALYSIS OF FAULTS IN GFM3.0

- (1) Are the data used to define faults at the surface and in the subsurface in GFM3.0 deemed appropriate and sufficient for this purpose?

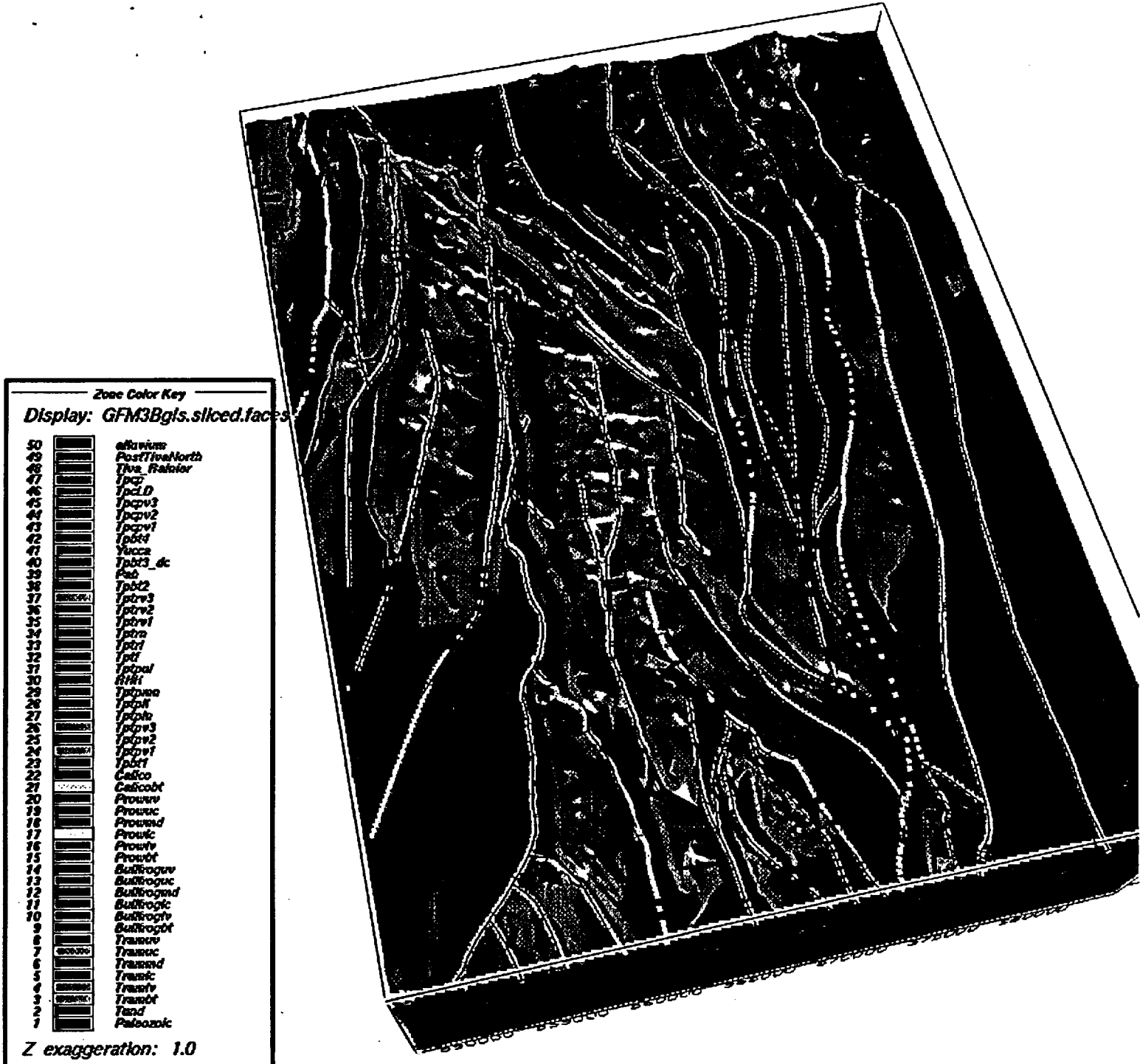
Surface data - Fault trace information derived from the geologic map of Day, et al. (1997) was used to define locations of faults at the surface in GFM3.0. Use of these data resulted in realistic representation of variations in strike of mapped faults and reasonable representation of strike of inferred faults beneath alluvium. Figure 1 illustrates the fault trace data from the original GFM3.0 database that were derived from the geologic map of Day, et al. (1997), compared with locations of surface fault trace lines actually contained in GFM3.0.

Subsurface data - Since borehole control points generally do not exist for defining dips of faults in the subsurface at Yucca Mountain (YM), dip lines generated from surface measurements of fault dips were used in conjunction with surface fault trace information to construct 2-dimensional (2D) grid (.2grd) files for modeling fault surfaces at depth. The approach amounts to projecting surface dip measurements on faults to depth for specifying fault dips in the subsurface. Lacking borehole control data directly suggesting that faults were non-planar within the depth range covered by GFM3.0, this approach was used to represent major west-dipping, north-northeast striking, normal faults as essentially planar features extending to the base of GFM3.0 (i.e., 8000 feet below sea level). A planar fault model is one possible interpretation suggested for subsurface geometry of west-dipping, north-northeast striking faults at YM (Brocher, et al, 1998). This subsurface fault geometry for YM proper is derived from the regional tectonic model for planar faulting at depth. A regional alternative tectonic model related to development of faults which are curved (i.e., listric) at depth at YM (Young, et al, 1992) is not considered in GFM3.0. Point 6(d) discusses observations specifically related to this alternative tectonic model, however.

Northwest-trending, strike-slip faults are planar and essentially vertical in GFM3.0. Certain minor west-dipping faults that are planar in the model intersect major structures and are truncated at the line of intersection rather than extending to depth. East-dipping, planar faults also intersect west-dipping, normal faults and are truncated at the line of that intersection above the base of GFM3.0. Fault Splay S off the east side of the Solitario Canyon fault is modeled in GFM3.0 as genuinely non-planar with a geometry and line of intersection with the Solitario Canyon fault similar to that of modified fault surface Ironw3 generated for this review of GFM3.0 (See Questions 4 and 5 below).

In summary, the data used in GFM3.0 to define fault surfaces from ground level to depth were appropriate and sufficient for constructing faults in the model. Fault traces and dip lines were used to construct fault surfaces as 2D grid (.2grd) files because borehole information does not exist for defining dips of faults in the subsurface. Fault surfaces are commonly planar in GFM3.0 and clipped with polygon (.ply) files as appropriate for limiting extent of a fault based on length of its surface trace. Fault trace data (as a .dat file) and polygon files (as .ply files) were provided in the GFM3.0 digital database along with all 2D grid (.2grd) files constructed for fault surfaces. Dip line files were not provided but are available from DOE should it be desired to examine these data. It was not necessary to peruse the dip line data files for this review of GFM3.0 since the fault surface dips modeled at depth reflect surface field measurements projected to depth.

Figure 1. Fault trace data points (yellow) from the original GFM3.0 database compared with fault trace lines (black) contained in GFM3.0



(2) Do fault traces and fault surfaces as modeled in GFM3.0 fit the input data?

Fault traces and fault surfaces included in GFM3.0 fit the field-based input data closely. Faults contained in GFM3.0, generated as polygon-clipped 2D grids as described above under Question 1, generally match well with mapped fault traces (Figure 1) and known near-surface dip angles of faults. Because borehole data do not exist for construction of refined 2D grids for the fault surfaces, fault traces and dip lines were used to generate fault surfaces in the model with the result that major west-dipping normal faults are represented as planar structures extending to the base of the model at -8000 feet. (However, see observations 6(f) and 6(h) below.)

(3) Were all data essential for constructing GFM3.0 included in the data files that accompanied the model?

All data essential for calculating 3D structure models (i.e., models illustrating fault surfaces, fault blocks, zone surfaces, and zone blocks), using Geologic Structure Builder (GSB), are available to NRC staff. The data were either included in the database originally or provided immediately by R. Clayton upon request when determined to be missing. Consequently, the master sequence (.seq) file developed by R. Clayton and provided with the original database was successfully used after minor editorial modifications to reconstruct .faces files for fault surfaces and fault blocks, as well as zone surfaces and zone blocks in the Computerized Risk Assessment and Data Analysis Laboratory (CRADAL) at NRC Headquarters. This .seq file contained information that defined 42 faults, 43 fault blocks, and 50 stratigraphic horizons (including alluvium) for GFM3.0. The editorial changes to the original master sequence (.seq) file included renaming certain files and rearranging locations of others to be able to access those essential for construction of .faces files for fault surfaces and fault blocks. The complete set of data files may be accessed by NRC users, since these files occur in the GFM3.0 database in the CRADAL.

In summary, all data essential for constructing GFM3.0 were either included in the data files which originally accompanied the model or provided immediately by R. Clayton once determined to be missing. To determine that all data essential for constructing GFM3.0 were lodged in the database, recalculation of .faces files was undertaken for fault surfaces and blocks and zone surfaces and blocks using a master sequence (.seq) file that was only slightly modified from the original. Figures 2 through 4 illustrate reconstructed .faces files for fault surfaces and fault and zone blocks and also show the 42 faults, 43 fault blocks, and 50 stratigraphic horizons included in GFM3.0.

(4) Are there alternative interpretations of the fault data suggesting that different representations of subsurface fault geometry may be reasonable to incorporate into GFM3.0?

The subsurface fault geometry represented in GFM3.0 exercises the interpretation that west-dipping, north-northeast trending faults are planar to depth. An alternative interpretation for subsurface fault geometry based upon concepts developed at CNWRA (Ferrill et al, in review, b) involves some structures developing as oblique faults in a relay ramp or as a connecting fault system, such that they merge with or terminate against major faults within the depth range of GFM3.0 (i.e., at some depth above -8000 feet). For example, faults Ironw1, Ironw2, and

Figure 2. Recalculated .faces file for fault surfaces showing that data in the GFM3.0 database are complete and permit construction of this file

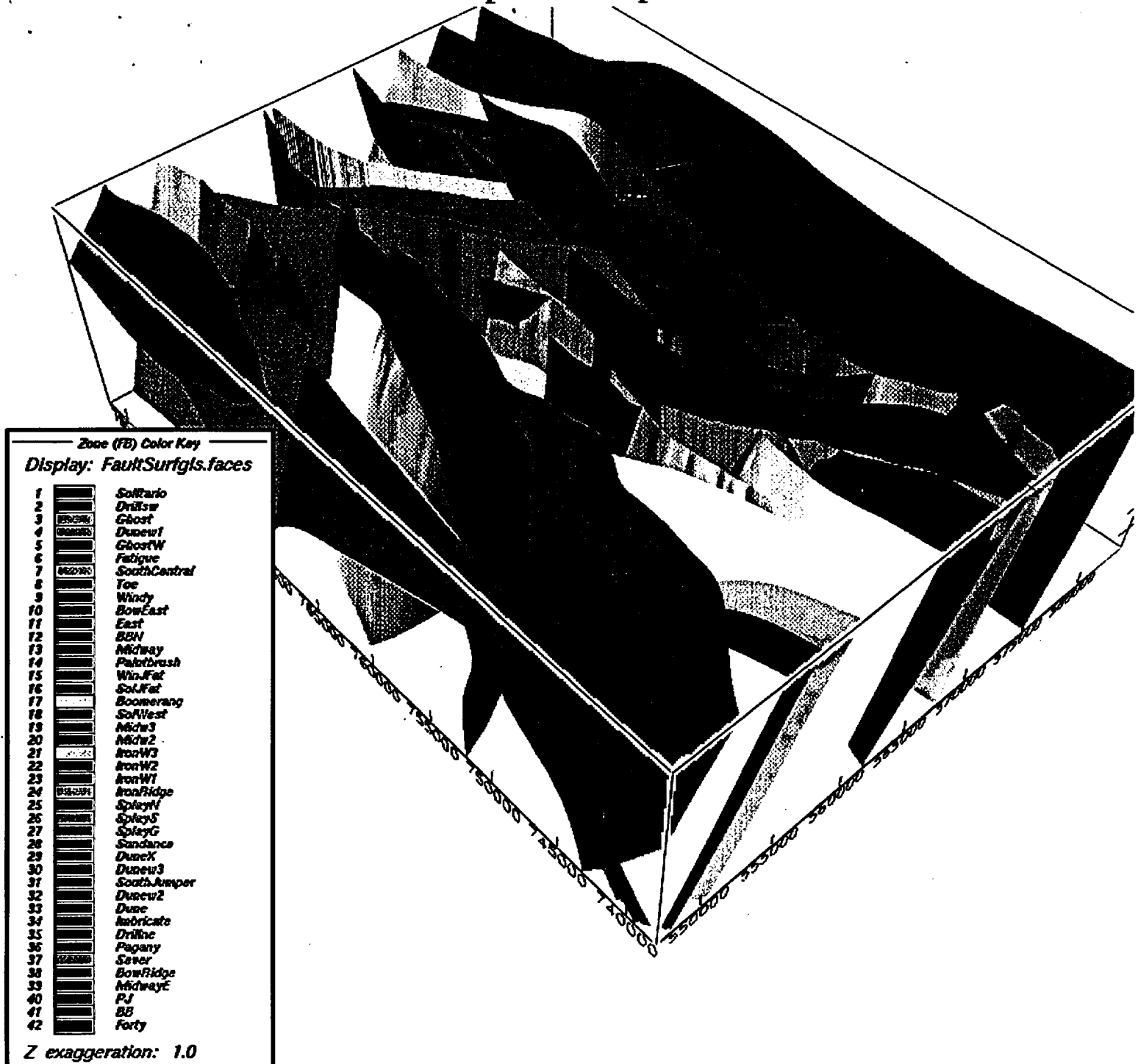


Figure 3. Recalculated .faces file for fault blocks showing that data in the GFM3.0 database are complete and permit construction of this file

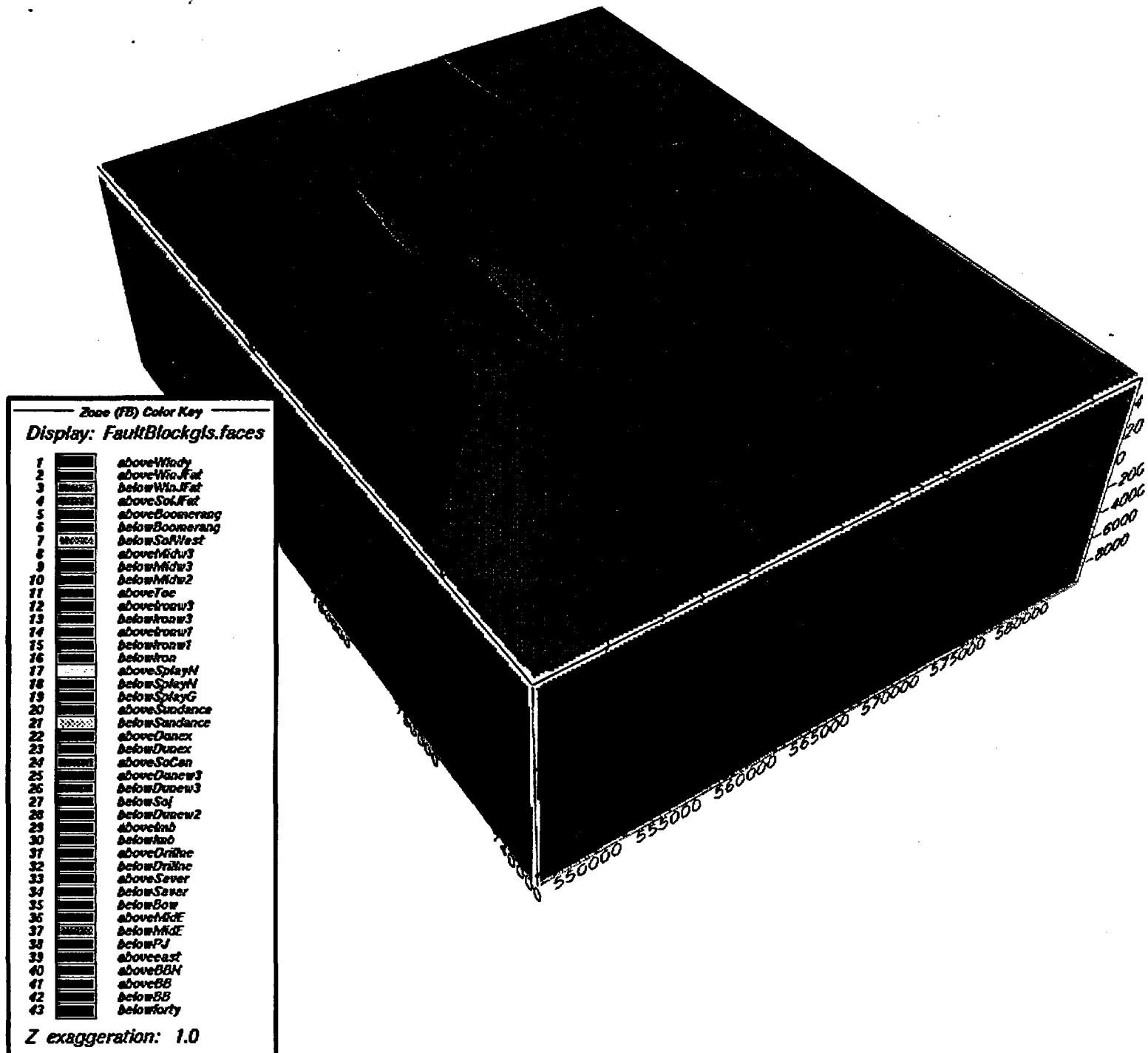
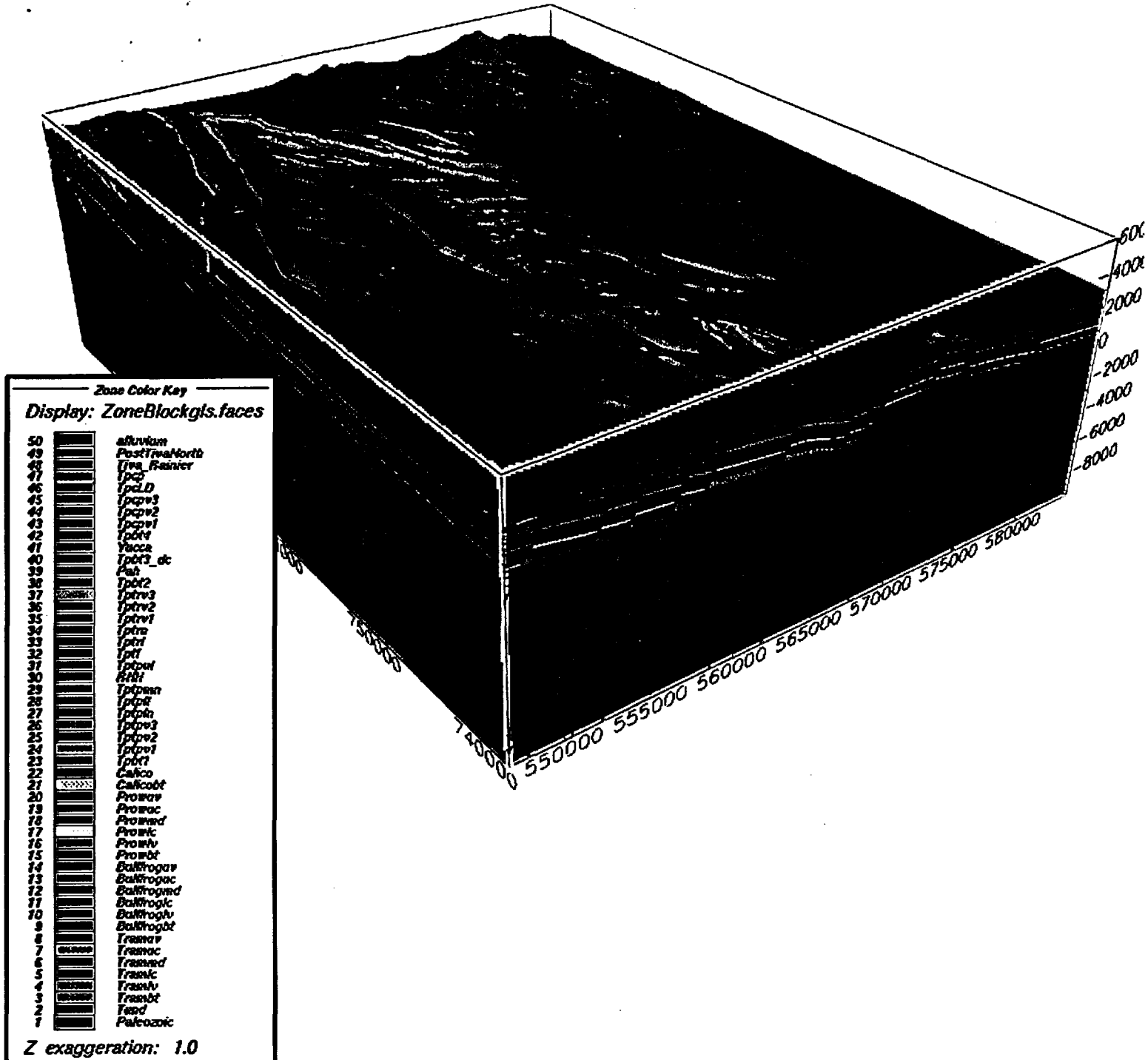


Figure 4. Recalculated .faces file for zone blocks showing that data in the GFM3.0 database are complete and permit construction of this file



Ironw3, between the Iron Ridge and Solitario Canyon faults at Yucca Mountain, are included in GFM3.0 as planar structural features. These faults are alternatively interpreted by CNWRA staff as oblique faults in a relay ramp that merge with the Solitario Canyon fault at depth rather than extending to the base of GFM3.0 as planar features (Ferrill, et al, in review, b).

In summary, all major and most minor faults included in GFM3.0 are represented as essentially planar structural features extending to the base of the model at -8000 feet. Fault Splay S off the Solitario Canyon fault is included as a truly non-planar feature that intersects the Solitario Canyon fault well above the base of GFM3.0. The interpretation that certain other faults may also be non-planar features at depth is a reasonable alternative model for subsurface fault geometry that was not considered in GFM3.0.

- (5) Is it possible to incorporate reasonable alternative interpretations of subsurface fault geometry into GFM3.0, specifically the interpretation that certain faults are non-planar and merge with or terminate against major structures at depths of less than -8000 feet above the base of GFM3.0?

Faults Ironw1, Ironw2, and Ironw3, located in the southwestern corner of GFM3.0, were represented in the model as planar structures extending to the base of the model at -8000 feet. The subsurface geometry of fault Ironw3 in the "Ironw" system was successfully modified to generate a non-planar fault that terminated at a depth no greater than -2000 feet against the Solitario Canyon fault. This test illustrates that it is practicable to alter subsurface geometry of faults in GFM3.0 for incorporating alternative interpretations of fault geometry. Figure 5 illustrates the planar subsurface geometry of Ironw3 as originally represented in GFM3.0 along with non-planar fault Splay S. Figure 6 shows Ironw3 as modified for this test to terminate against the Solitario Canyon fault at a depth no greater than -2000 feet. Fault Splay S is included in the figure to show the similarity between the geometry of Splay S and modified Ironw3.

In summary, the result of this successful test illustrated by Figure 6 proves it is possible to modify GFM3.0 and incorporate alternative interpretations of subsurface fault geometry into the model. Although a detailed explanation of the steps necessary to generate modified fault surfaces is beyond the scope of this letter report, some words of caution are advised. When fault geometries are changed, before running the master sequence (.seq) file in GSB to generate modified .faces files for structure models, it may be necessary to rebuild the fault tree or re-grid horizons in the fault blocks. In particular, if the number of fault blocks is either reduced or increased, as is likely when removing an existing fault or adding a new one in the model, rebuilding the fault tree and re-gridding of horizons in the altered fault blocks are commonly necessary before the .seq file can be used in GSB to calculate .faces files for the suite of structure models (i.e., fault surfaces and blocks and zone surfaces and blocks).

- (6) What observations were made relative to representation of faults in GFM3.0 that may require further explanation or clarification?

- a. No northwest-trending structure is included along Antler Wash in the vicinity of borehole H-4 where hydrologic testing suggested some type of connection between H-4 and the C wells. No northwest-trending fault was included in Antler Wash because

Figure 5. Planar fault ironw3 (tan) as originally included in GFM3.0. Also shown are part of the Solitario Canyon fault (green) and Splay S

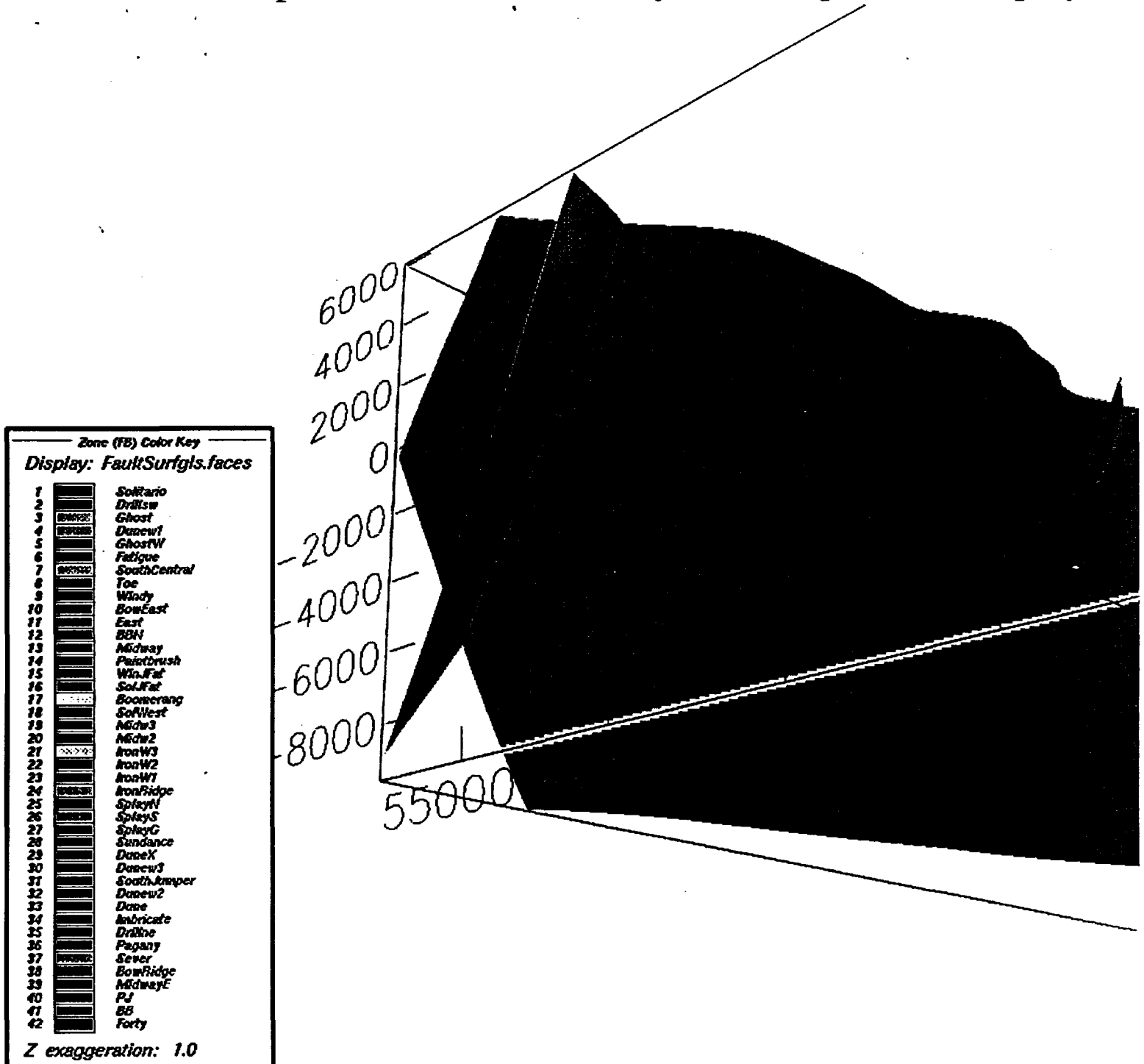
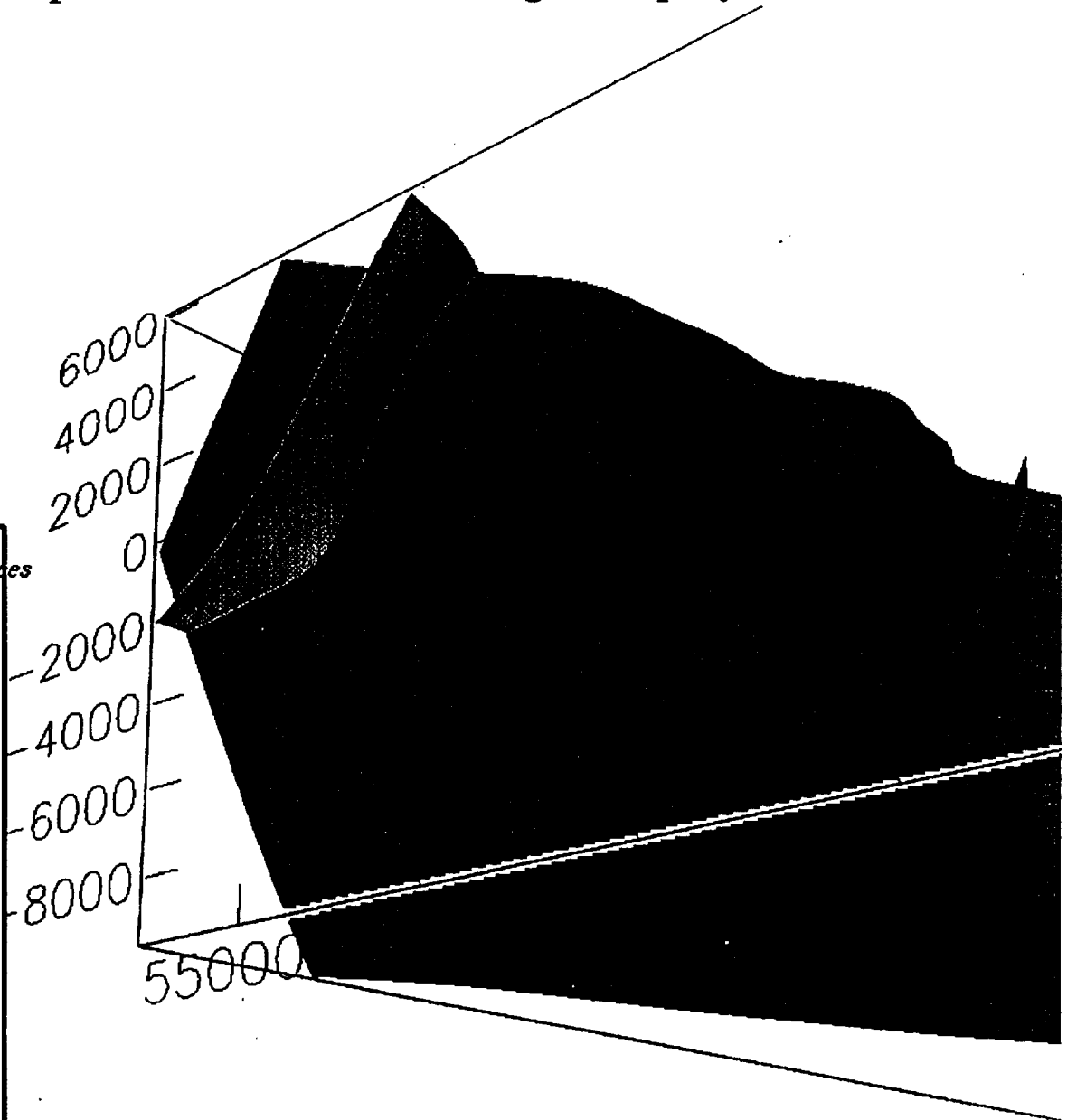
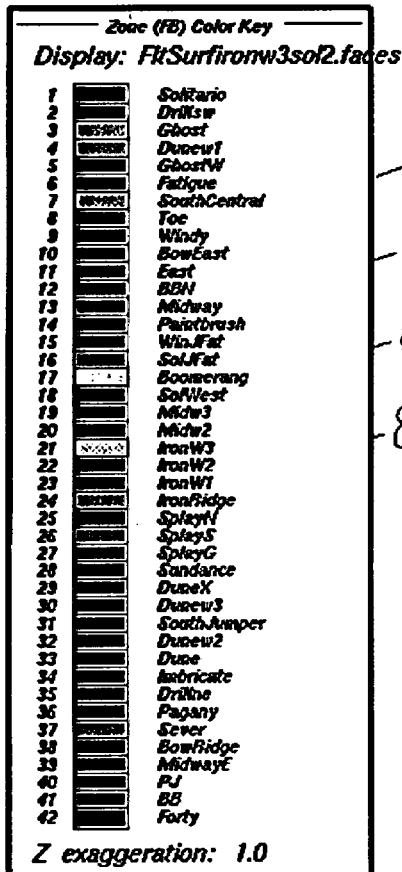


Figure 6. Fault Ironw (tan) modified to intersect the Solitario Canyon fault (green) no deeper than -2000 feet. Original Splay S is also shown



geologic mapping did not delineate such a structure in rocks at the head of the wash, although a dashed symbol for a northwest-trending fault in Antler Wash is shown on the geologic map of Day and others (1997). This could be rectified by adding this fault to GFM3.0, although, from H-4 southeast to the C wells, major north-northeast trending faults also occur so that the hydrologic connection is possibly a complex one, at best.

- b. The imbricate fault zone is presently modeled as a single fault. This representation could also be changed in the model if there is any need to capture more structural complexity in that zone.
- c. The Forty Mile Wash fault is included as a prominent structural feature in GFM3.0. Although the presence of this feature and the logic for its inclusion in GFM3.0 has been discussed with R. Clayton, with the history that exists since it was first proposed by Young, et al (1992) based on interpretations from balanced cross sections, the acceptance of the structure by the USGS could perhaps be clarified.

From examination of nine (9) cross sections taken directly from GFM3.0 at traverse locations indicated in Figure 7, additional observations were also made as follows. (Note that the fault labeled as "EHF" in Figure 7 and subsequent cross sections is fault "BowEast" in GFM3.0.)

- d. Folding developed in the hangingwall blocks of faults is generally attributed to a curved (i.e., listric) fault geometry at depth (Suppe, 1983; Dula, 1992). Sections 1 (Figure 8) and 8 (Figure 15) through the model appear to illustrate folding of units in hangingwall blocks although GFM3.0 is constructed with essentially planar faults. Explanation of why these units appear to be folded may be helpful. By some interpretations (e.g., Young, et al., 1992), at the depth to which the model was constructed (i.e., 8,000 feet below sea level), the Forty Mile Wash, Paintbrush Canyon, Midway Valley, and Bow Ridge faults would show curved trajectories.
- e. The Boomerang Point fault is shown as reversing displacement at depth in Sections 5 (Figure 12) and 6 (Figure 13). This may be due to model construction artifacts or potential uncertainty on the depth to the Paleozoic surface, so clarification may be helpful.
- f. The Dune Wash fault is shown to be truncated against the Ghost Dance fault in Section 5 (Figure 12) but not in Section 4 (Figure 11). This observation suggests a change in dip or "flexing" of the Dune Wash fault so some clarification may be useful.
- g. Many faults are shown with displacements across the Paleozoic surface that are generally greater than the displacement of the base of the younger Trambt. The exceptions to this are the Solitario Canyon fault in Sections 2 (Figure 9), 3 (Figure 10), 4 (Figure 11), and 9 (Figure 16) and the Forty Mile Wash fault in Section 9 (Figure 16). Increasing differential displacement with depth implies growth in at least the earlier Tertiary sequence, so it may be helpful to clarify whether implied growth is part of the premise for GFM3.0. These displacements for the Solitario Canyon and Forty Mile Wash faults are at the northern and southern edges of the model where well control is

GFM version 3.0

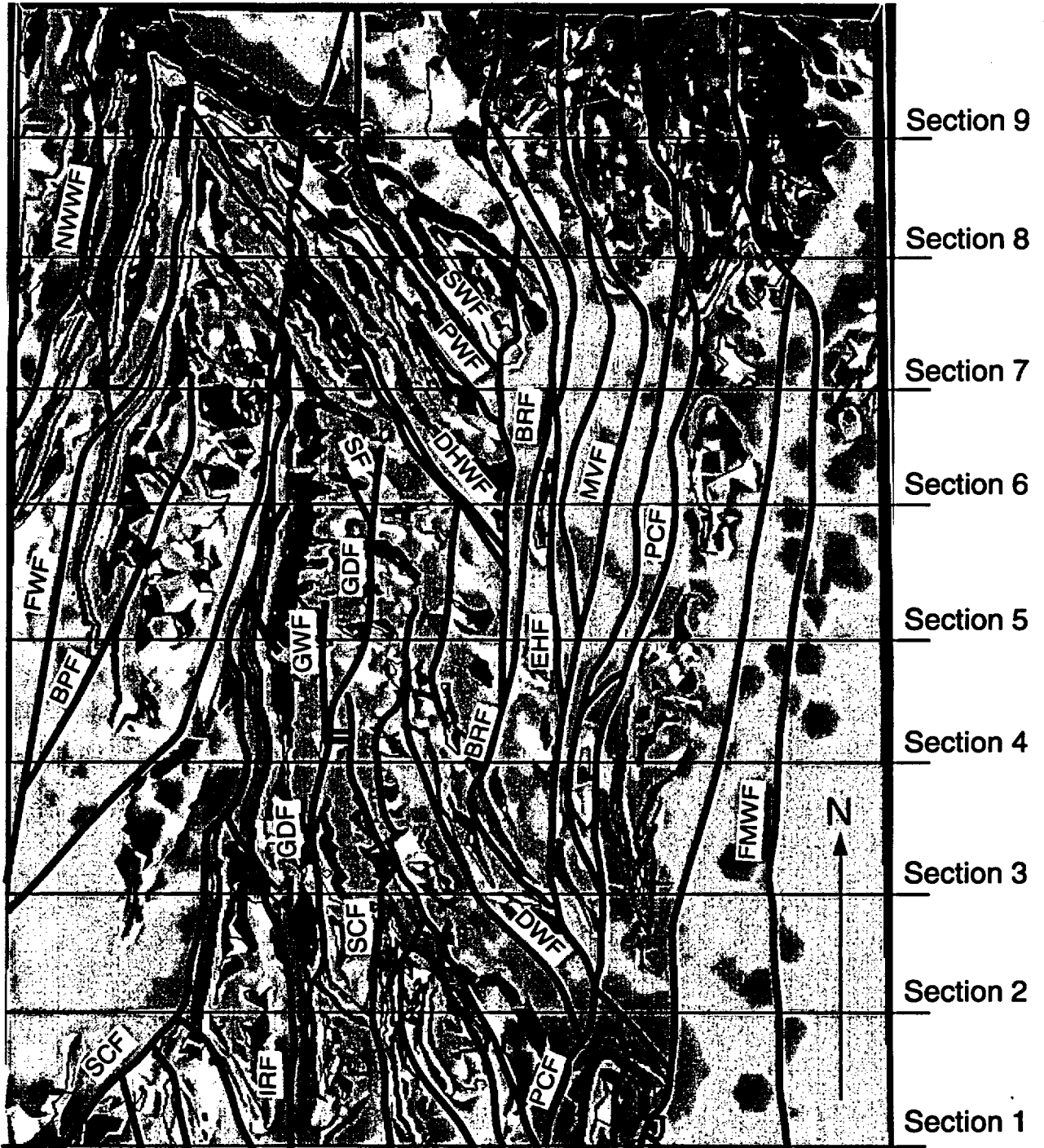


Figure 7 – Index map showing locations of sections 1 to 9 across GFM Version 3.0 as shown in figures 8 to 16.

Section 1

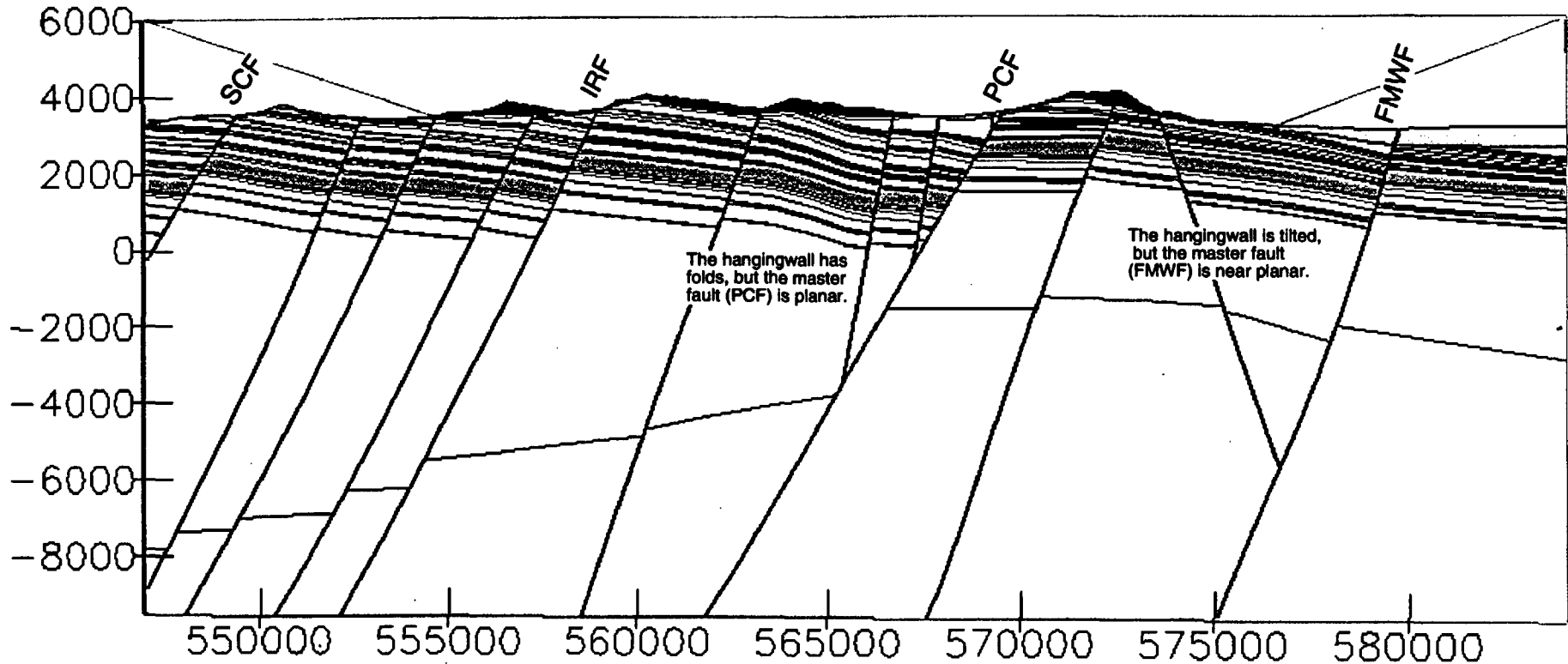


Figure 8 – Cross section 1. This section illustrates folding in the hangingwall of the PCF without curvature in the associated fault plane. Slight curvature of the FMWF may not be sufficient to produce tilting as shown in the hangingwall. See Figure 7 for location.

Section 2

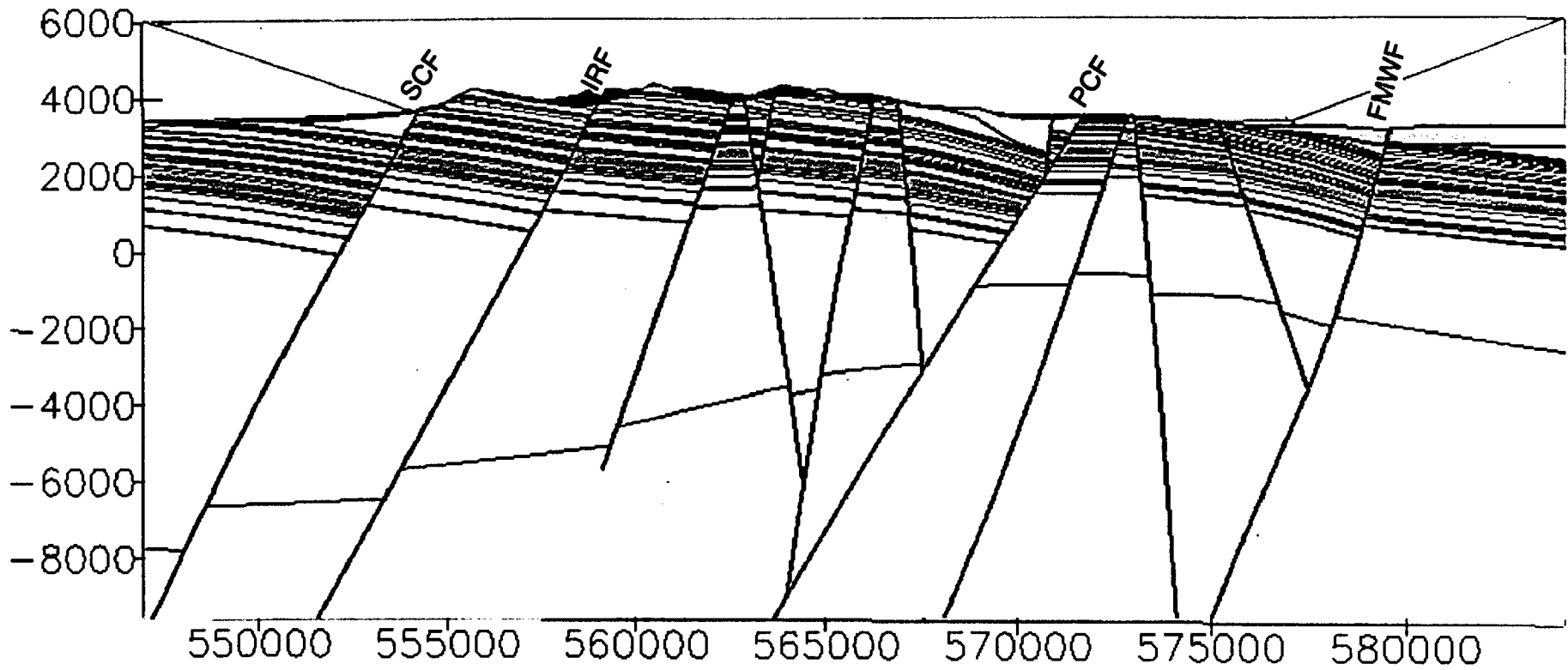


Figure 9 - Cross section 2. See Figure 7 for location.

Section 3

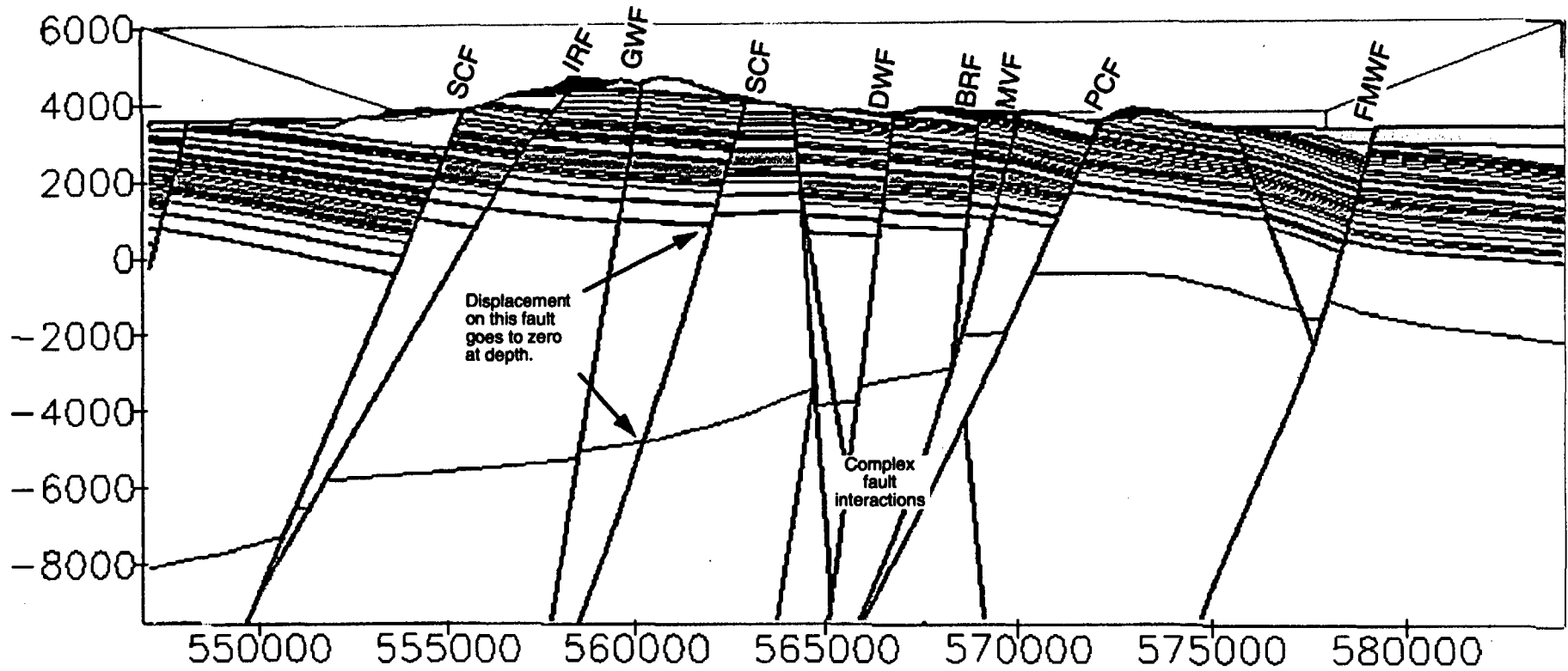


Figure 10 – Cross section 3 illustrates complex fault geometries, including fault displacement decreasing with depth (SCF), faults that are terminated updip by other faults, and crossing fault geometries. See Figure 7 for location.

Section 4

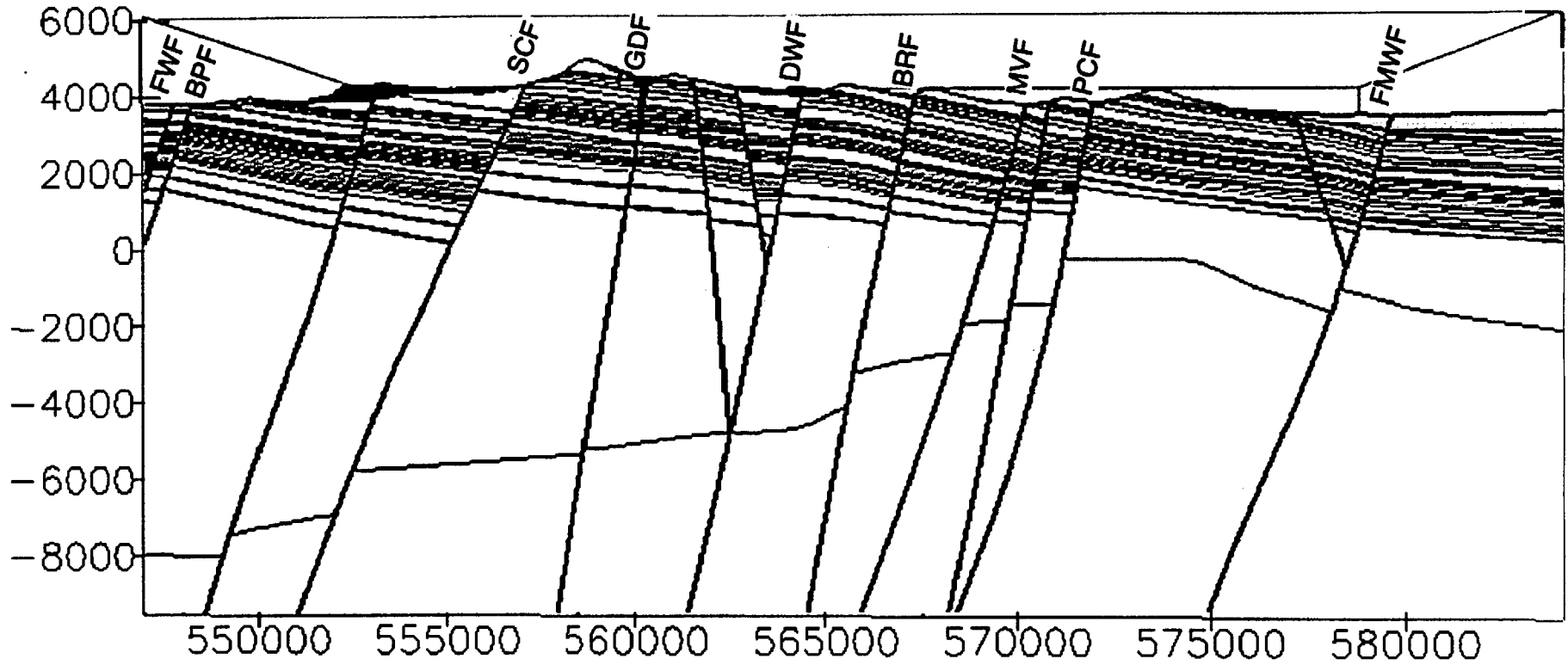


Figure 11 – Cross section 4. The DWF fault is continuous through model stratigraphy in cross section 4, and is discontinuous in cross section 5 (Figure 12). See Figure 7 for location.

Section 5

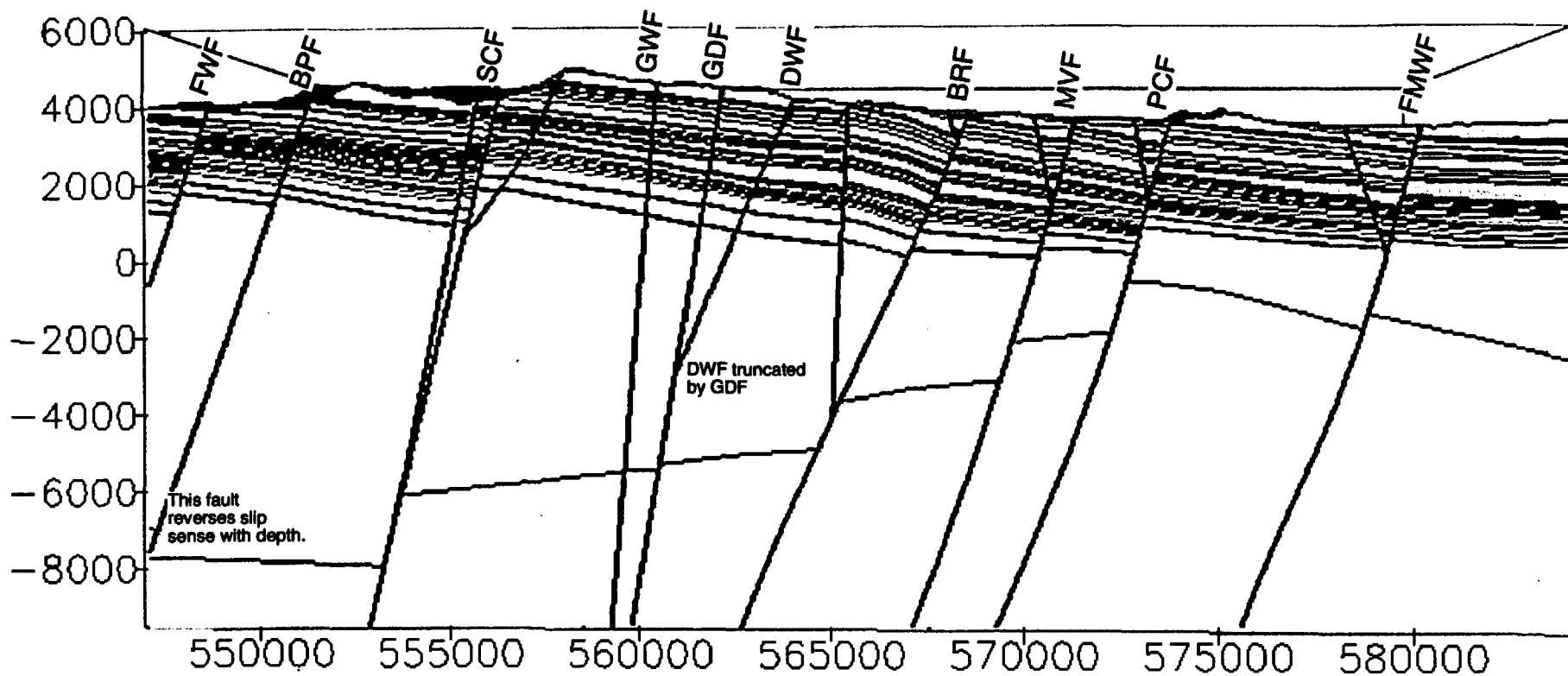


Figure 12 – Cross section 5 illustrating truncation at depth of DWF fault by GDF fault and reverse of slip sense with depth of BPF fault (see also Figure 13). Section 4 (Figure 11) shows DWF fault continuous through model stratigraphy. See Figure 7 for location.

Section 6

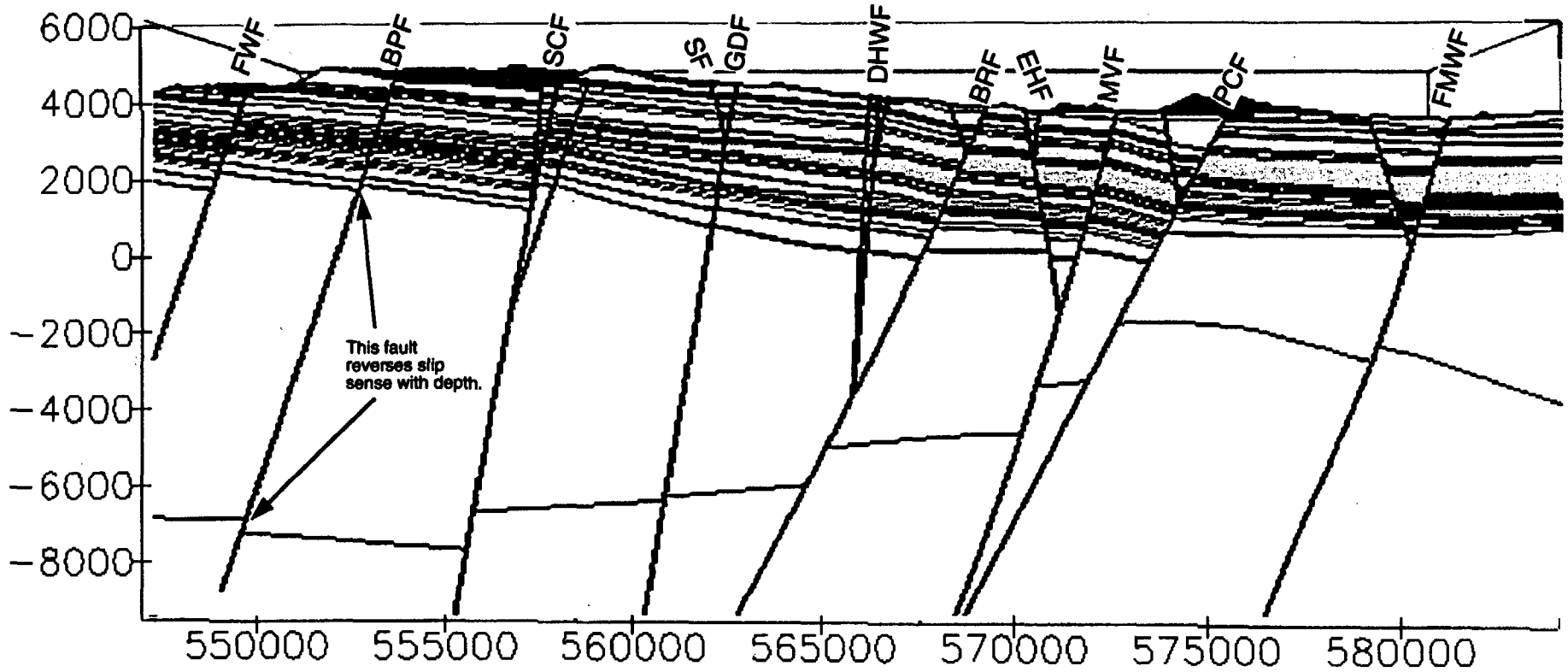


Figure 13 - Cross section 6 illustrating reverse of slip-sense at depth of BPF fault (see also Figure 12). See Figure 7 for location.

Section 7

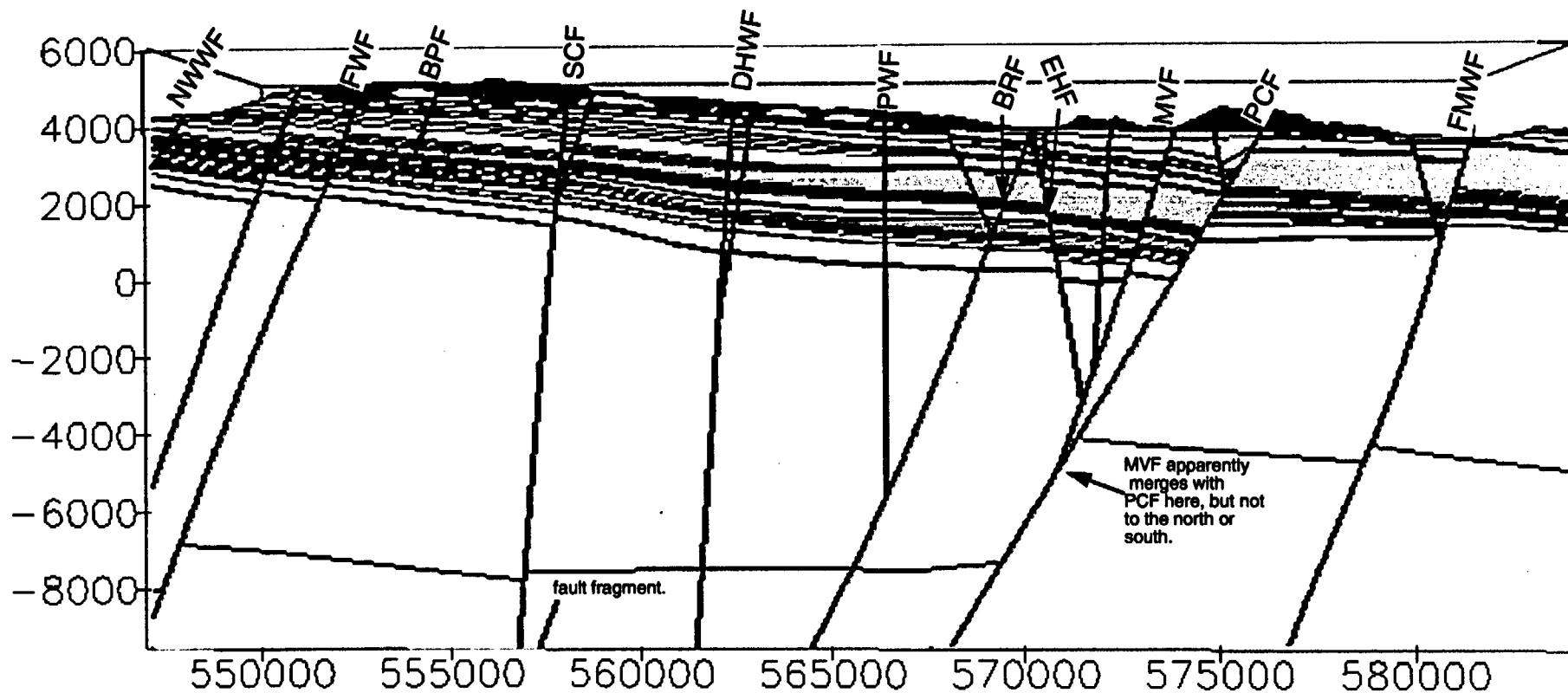


Figure 14 - Cross section 7 illustrates merging of MVF with PCF at depth. These faults do not merge in cross sections 6 (Figure 13) and 8 (Figure 15). Fault fragment terminates updip. See Figure 7 for location.

Section 8

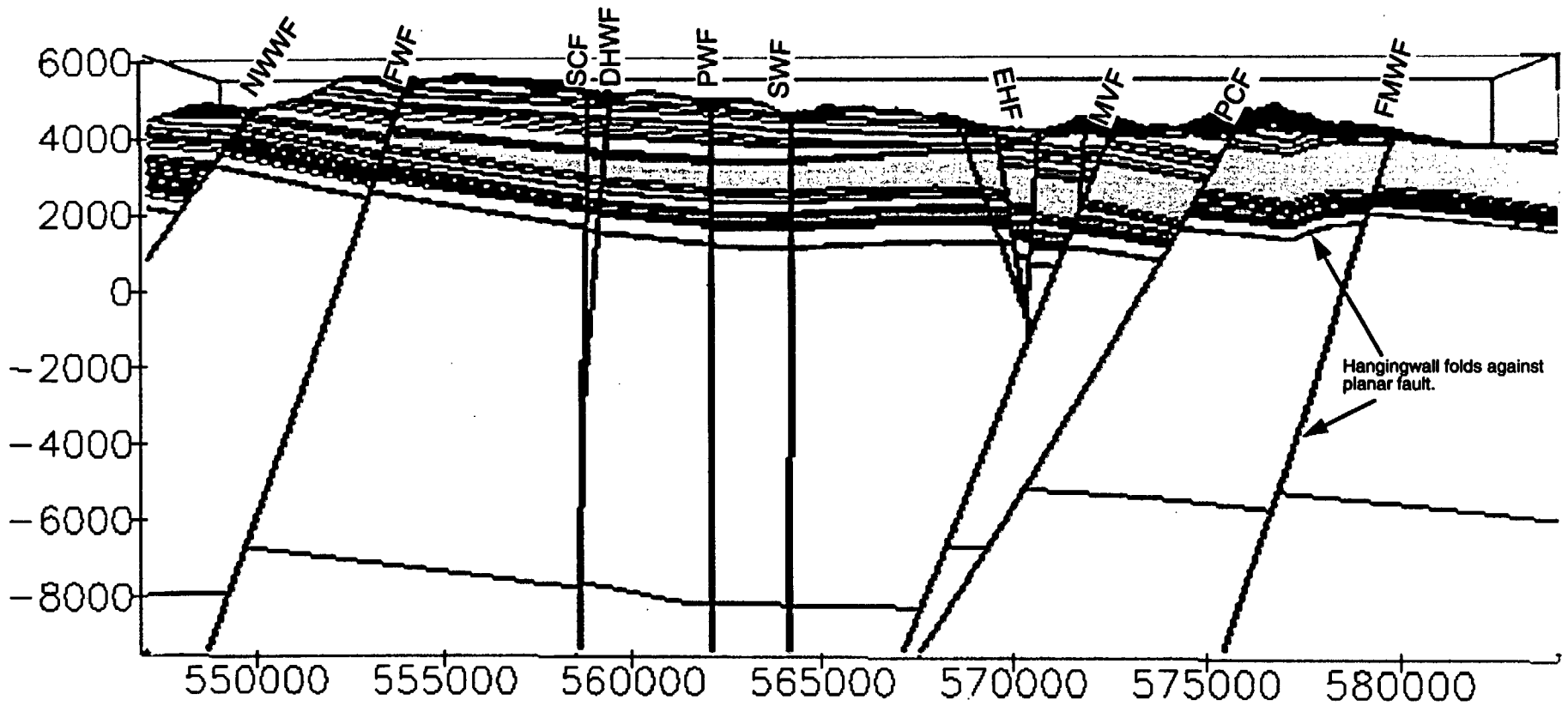


Figure 15 - Cross section 8 illustrating folded beds in the hanging wall of FMWF without curvature of associated fault surface. See Figure 7 for location.

minimal and may reflect sparse data. Effects of sparse data may also be reflected in GFM3.0 as greater discrepancies between the data and the extrapolations made by EarthVision software for depths to stratigraphic horizons (See Figure 5 in Part I). Consider clarifying what uncertainties are associated with the estimates to the depth of the Paleozoic surface.

In Yucca Flat, the mean depth differences between depth estimates based on gravity and actual tags of the Paleozoic rock surface at 38 drill holes was 30m +/- 88m. (Brethauer, et al., 1981). At Yucca Mountain, only a few boreholes can be used to define the Paleozoic surface. (Ue25 p-1 is the only borehole that penetrates this surface. A few other holes, such as G-1 and Gu-3, while not penetrating the surface do constrain its depth.) This information suggests that, as a minimum, only offsets greater than 100 m can be used as control for the location of faults intersecting the Paleozoic surface, and displacements of less than 100 meters may be artifacts of model construction. Consider clarifying whether artifacts of modeling are an influence in this case.

- h. Complex interactions between faults with opposing dip (e.g., Section 3, Figure 10) are likely in the Yucca Mountain area (Brocher, et al. 1998) and may be important influences on groundwater flow (Ferrill, et al. 1998). Variable displacement values between different units at the same position along a given fault and beheaded faults without a continuation across the offsetting fault are examples of complex fault interactions. Consider clarifying whether these complex interactions are real or modeling artifacts.

Section 9

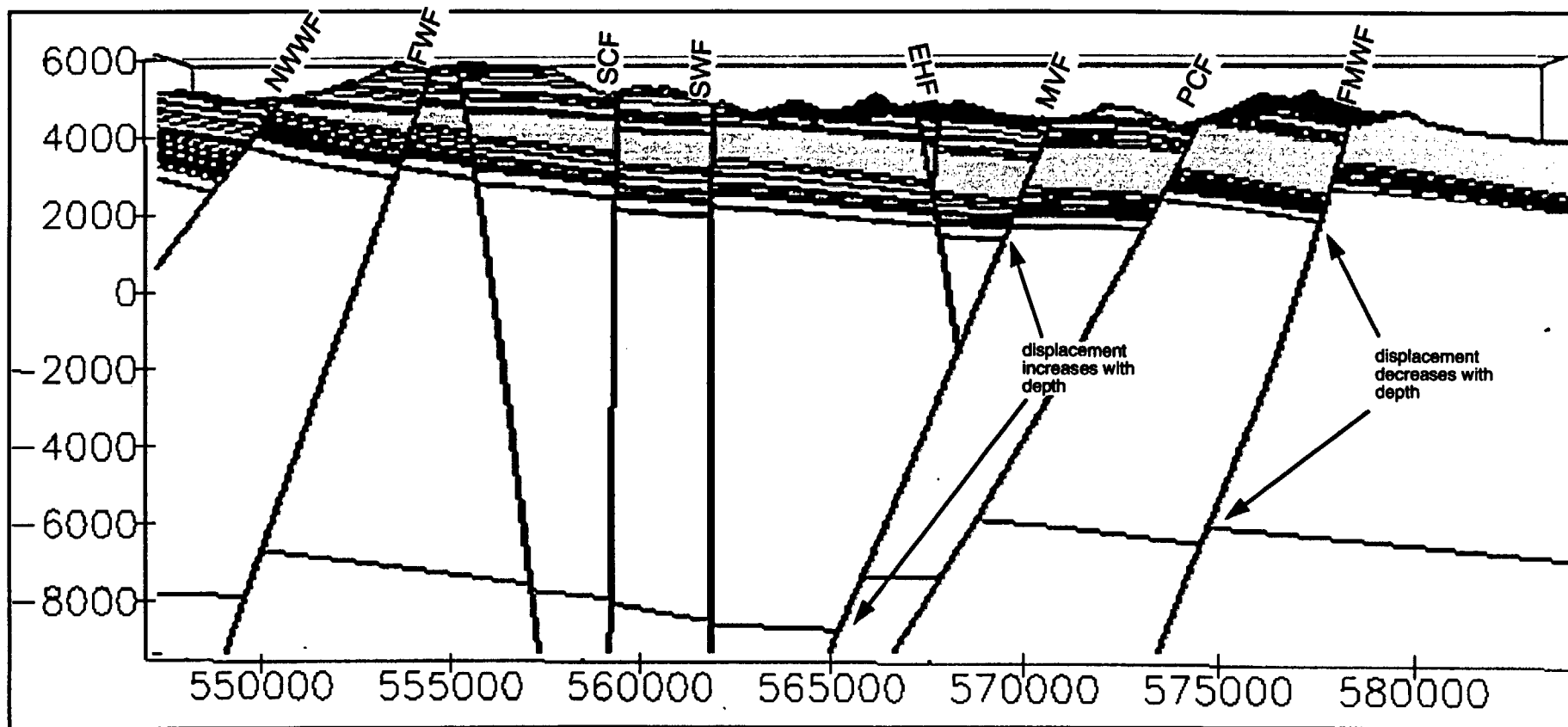


Figure 16 - Cross section 9 illustrating displacement increasing with depth along MVF and decreasing with depth along FMWF. See Figure 7 for location.